NACA

RESEARCH MEMORANDUM

MOTION OF A TRANSONIC AIRPLANE NOSE SECTION WHEN JETTISONED AS DETERMINED FROM WIND-TUNNEL INVESTIGATIONS ON A $\frac{1}{25}$-SCALE MODEL

By Stanley H. Scher and Lawrence J. Gale

Langley Aeronautical Laboratory
Langley Air Force Base, Va.

NATIONAL ADVISORY COMMITTEE FOR AERONAUTICS

WASHINGTON

May 26, 1950

NATIONAL ADVISORY COMMITTEE FOR AERONAUTICS

RESEARCH MEMORANDUM

MOTION OF A TRANSONIC AIRPLANE NOSE SECTION WHEN JETTISONED AS DETERMINED FROM WIND-TUNNEL INVESTIGATIONS ON A $\frac{1}{25}$-SCALE MODEL

By Stanley H. Scher and Lawrence J. Gale

SUMMARY

An investigation has been conducted with a $\frac{1}{25}$-scale model in the Langley 300 MPH 7- by 10-foot tunnel, the Langley free-flight tunnel, and the Langley 20-foot free-spinning tunnel to determine the path and motion of a transonic airplane nose section when jettisoned. The investigation included determination of the probable accelerations that would act on a pilot in the jettisoned nose section.

The results of the investigation indicate that when an airplane nose section without stabilizing fins is jettisoned, it will have an inherent tendency to turn away from a stable nose-first attitude and therefore cause an increased drag which may cause high accelerations on the pilot within the nose section. The results also indicate that forcible forward ejection of a fin-stabilized jettisonable nose section may be necessary to assure clean separation of the nose from the rest of the airplane and to force the nose forward of a region where high negative lift due to the nearness of the rear body may cause high accelerations on a pilot.

INTRODUCTION

A proposed method of providing for emergency pilot escape from high-speed airplanes consists of jettisoning the nose section of the fuselage clear of the remainder of the airplane, with the break-off station just rearward of the pilot's station; the pilot leaves the nose section after it has decelerated to a safe speed.

In previous investigations (references 1 and 2), it was indicated by tests of the nose alone that because of inherent instability of the nose section, the pilot will be subjected to high accelerations unless the nose is stabilized so that it will travel in a nose-first attitude. The adequacy of fins for this purpose, both at low speeds and at supersonic speeds, has been indicated in references 1 to 3. Also, the forces and moments acting on a nose when in the vicinity of the rear portion of the airplane model have been measured (reference 4).

The purpose of the present investigation was to determine the path and motion of a nose section both with and without fins immediately after its release from an airplane and to ascertain the accelerations acting on the pilot resulting from the behavior of the nose. For the investigation, a dynamic model of the nose section of a $\frac{1}{25}$-scale model representative of a transonic airplane was released from the rest of the model which was fixed in various attitudes in the Langley 300 MPH 7- by 10-foot tunnel, the Langley free-flight tunnel, and the Langley 20-foot free-spinning tunnel. A few nose releases were also made for various conditions of the model descending freely in the spin tunnel.

SYMBOLS

m	mass, slugs
I_X, I_Y, I_Z	moments of inertia about X (longitudinal), Y (lateral), and Z (normal) body axes, respectively, slug-feet^2
V	airspeed, feet per second
ρ	density of air, slugs per cubic foot
s	displacement, feet
g	acceleration of gravity (32.17 ft/sec^2)
t	time, seconds
R	scale ratio, ratio of any dimension of full-scale nose section to corresponding dimension of model nose section

Subscripts:

v	vertical component

h horizontal component

m model

fs full scale

APPARATUS AND METHODS

Model

The model used in the nose-release investigation was considered to be a $\frac{1}{25}$-scale model representative of a transonic airplane. A three-view drawing of the model is shown in figure 1 and a photograph of the model is shown as figure 2. For the investigation, the nose of the model was made removable at a station 4 inches (100 in., full scale) rearward of the front end of the fuselage. Sketches of the nose section with and without the stabilizing fins are presented in figure 3. For the nose releases from the fixed model, the nose was ballasted with lead weights to approximate dynamic similarity to the full-scale nose section at an altitude of 15,000 feet (ρ = 0.001496 slug per cu ft). For the nose releases from the model when descending freely in the Langley 20-foot free-spinning tunnel, both the nose and the complete model were dynamically ballasted. The mass data for the nose section model and for the complete airplane model in terms of full-scale values are presented in table I.

Wind Tunnels and Tests

For the nose-release tests conducted in the Langley 300 MPH 7- by 10-foot tunnel, which is a horizontal atmospheric wind tunnel, the model was attached to a steel bracket mounted to the tunnel ceiling. The nose was held in place by an electromagnet in the model and was released when desired by opening the circuit that supplied current to the electromagnet. Releases were made for the nose with and without fins with the airplane model at 0° angle of attack for tunnel airspeeds ranging from 60 miles per hour to 150 miles per hour. Also, a few releases were made with the airplane model at 5° and -5° angle of attack for the fin-stabilized nose at 150 miles per hour. The full-scale airspeed range corresponding to the tunnel airspeed range would be from 300 miles per hour to 750 miles per hour (neglecting compressibility effects), based on the following relationship from reference 5:

$$V_{fs} = \sqrt{R}V_m$$

A complete description of the Langley free-flight tunnel and its operation is given in reference 6. This tunnel can be tilted so that its air stream is deflected up or down from horizontal, and it was therefore a convenient tunnel in which to make nose-release tests from conditions simulating gliding and climbing flight of the airplane. For these tests the model was held in place by stout cords fastened to the walls and ceiling of the tunnel and the nose section was released when desired by pulling out two light strings which held it in place. These tests were conducted only for the nose without fins and with the airplane model at simulated glide path angles of 0° (level flight), 10° climb, and 30° dive, and for angles of attack of 0° and 8°. All tests in the Langley free-flight tunnel were made at a tunnel airspeed of 56 miles per hour (280 mph, full scale).

The Langley 20-foot free-spinning tunnel is a vertical tunnel with a vertically rising air stream. The operation of the tunnel is generally similar to that for the Langley 15-foot free-spinning tunnel as described in reference 7. Nose-release tests were conducted for the nose with and without fins while the model was mounted in the tunnel at 0° angle of attack simulating vertical nose-down flight. Also, a few free tests were made with the complete dynamic model for which the nose was jettisoned while the model was spinning freely in the tunnel or in a condition simulating uncontrollable free descent of the airplane following loss of a wing or of the tail. For these free tests, the model was launched by hand into the vertically rising air stream. A remote-control magnetic device in the model was used to release the nose. The tunnel airspeed in the tests was approximately 35 miles per hour (175 mph, full scale).

Motion pictures were made of all the tests. The camera speeds used were approximately 100, 48, and 64 frames per second for the tests in the Langley 300 MPH 7- by 10-foot tunnel, the Langley free-flight tunnel, and the Langley 20-foot free-spinning tunnel, respectively. In the Langley 300 MPH 7- by 10-foot tunnel, a time indicator calibrated to 0.01 second was filmed simultaneously with the nose-release tests in order to obtain an accurate determination of the camera speeds.

Analysis of Tests

From the motion pictures of the tests, the path and motion of the nose section after each release were plotted. Curves were then drawn showing the horizontal and vertical displacements with time of a point at the pilot's head as the nose moved in the air stream. The relationships used in obtaining the full-scale displacement-time curves for the nose section were obtained from reference 5 and are as follows:

$$s_{fs} = Rs_m$$

and

$$t_{fs} = \sqrt{R}t_m$$

The first and second differentiations of the displacement-time curves were obtained graphically to show the full-scale horizontal and vertical velocities and accelerations (with respect to ground) at the pilot's head. The horizontal and vertical accelerations obtained were resolved trigonometrically into components acting along the backbone of the pilot (called longitudinal accelerations) and from the front to the back of the pilot (called transverse accelerations). These accelerations are compared with data in reference 8, which gives information on human tolerance to accelerations, although it has been indicated that recent experience by the Air Force points to the possibility that man's tolerance to negative accelerations along the backbone may be greater than the limits shown in reference 8. Although the graphically obtained accelerations presented herein are believed to be accurate only within ±2g, it is felt nevertheless that the results obtained are an accurate qualitative indication of whether or not the pilot is likely to encounter large accelerations.

RESULTS AND DISCUSSION

The results have not been corrected for Mach number and Reynolds number effects and therefore cannot be taken as quantitatively correct. It is believed, however, that they give a qualitative indication of results that would be obtained at large Reynolds numbers and at supersonic speeds.

Nose without Fins

When released in the Langley 300 MPH 7- by 10-foot tunnel, the nose without fins pitched downward about its Y-axis (counterclockwise when viewed from the left wing) as it dropped below and traveled behind the restrained airplane model. The nose usually made about one turn before it went out of camera view or hit in a safety net mounted downstream in the tunnel. Motion-picture film strips and plots of the variations of displacement, velocity, and acceleration with time obtained for typical releases of the nose section are presented in figures 4 to 9. These tests were made at airspeeds corresponding to full-scale true airspeeds at 15,000 feet of 400 miles per hour and 625 miles per hour as indicated on the figures. The accelerations which would act along the pilot's backbone during the releases are presented in figures 6 and 9 and it can be seen that after the releases at 400 miles per hour and 625 miles per hour a pilot would encounter negative accelerations (blood mass shifting toward head) of 8g for 0.16 second and 12g for 0.07 second, respectively, which, according to reference 8, are more severe than a man can tolerate. It is believed that the high accelerations were due primarily to an increase in drag resulting when the jettisonable nose turned away from a nose-first attitude. This is indicated by the results in figures 6 and 9 which show that the large accelerations were existent by the time the model had turned to an attitude approximately at right angles to its forward motion. Similar results have been indicated at supersonic speeds (reference 2) when models of isolated jettisonable nose sections without fins were projected in the Langley free-flight apparatus.

Supplementary tests made on an isolated dynamic model of a nose section mounted free to pitch have indicated that at high forward speeds a nose section will not tumble continuously end over end, as was indicated as possible in reference 1, but would trim approximately at right angles to its linear path. Static force tests made on a nose also have indicated that trim would occur at approximately 90° to its path (reference 4). It thus appears that although a full-scale nose section without fins may not tumble at high forward speeds, it will nevertheless trim across its path, thus giving rise to large accelerations.

When the nose was released in the Langley free-flight tunnel from conditions simulating level and climbing flight at both 0° and 8° angle of attack, the motion of the nose was generally similar to its motion when released in the Langley 300 MPH 7- by 10-foot tunnel at the lower airspeeds. However, when released during simulated 30° gliding flight the nose pitched upward (clockwise when viewed from the left wing) instead of downward and collided with the front of the rest of the model. It is recognized that such a collision may not necessarily occur following jettisoning of the full-scale nose inasmuch as the rear body would probably not continue flying with unchanged speed and direction such as was simulated during the nose releases from the mounted model. However, calculations were made of the accelerations which would have acted on a pilot due to the nose striking the rear body and to the ensuing rotation and the results indicated that the pilot would be exposed to a negative acceleration of approximately 10g for 0.03 second along the backbone. Reference 8 indicates that a man can tolerate a negative acceleration of 10g for only 0.007 second. Photographs of the nose as it was released and as it struck the rear body are shown in the motion-picture strips of figure 10.

When the nose was released at low speed while the airplane model was mounted in a vertical nose-down attitude in the Langley 20-foot free-spinning tunnel, the nose, as was expected, went into an end-over-end tumbling motion similar to that obtained with the larger model of the nose investigated previously (reference 1). When released from the free model, the nose also started tumbling and sometimes struck the wing or the tail soon after being released. The collisions could probably have been avoided by jettisoning the nose with a forcible forward ejection. The nose is shown striking the wing of the free airplane model after being released during simulated uncontrollable flight following loss of the tail in the motion-picture strips of figure 11.

Fin-Stabilized Nose

When released from the airplane model mounted at 0° or -5° angle of attack in the Langley 300 MPH 7- by 10-foot tunnel for all the test airspeeds, the finned nose traveled in nose-forward stable flight as it went below and behind the restrained airplane model. When the airplane model was at 5° angle of attack, the stable nose traveled above the rear body instead of below it. The results indicated that for the higher airspeeds, the pilot in the fin-stabilized nose would be subjected to high negative accelerations along his backbone when the nose went below the rear body. When the nose went above the rear body, the accelerations obtained would be positive along the pilot's backbone. Motion-picture film strips and plots of the variations of displacement, velocity, and acceleration with time obtained from the tests in which the fin-stabilized nose went below the rear body after being released at airspeeds corresponding to full-scale true airspeeds at 15,000 feet of 400 miles per hour and 625 miles per hour are presented in figures 12 to 15. Because the nose was stable, the accelerations a_v and a_h in figures 13 and 15 represent accelerations acting along the backbone (longitudinally) and transversely, respectively, through the pilot's body. It can be seen in figure 15 that after the nose release at 625 miles per hour (full-scale airspeed), a pilot would encounter a high negative longitudinal acceleration of 12g for 0.04 second due to the rapid downward movement of the nose. The rapid downward movement was probably caused by the development of a high negative lift on the nose just as the nose started to slide down from the rear body. Such a region of high negative lift, and resulting large acceleration, has previously been shown to exist by the results of calculations based on force tests on a large scale model of the nose section in the presence of the rear body (reference 4). It appears, therefore, that it may be necessary to eject forcibly a fin-stabilized nose section forward of the region where high negative lift due to the nearness of the rear body might cause high accelerations on the pilot. In regard to the transverse accelerations which may act on a pilot in a fin-stabilized nose, the results on figures 13 and 15 indicate that these accelerations are small and well within the limit that a man can tolerate. These small transverse accelerations are in agreement with results obtained when fin-stabilized models of isolated nose sections were fired (reference 2) at Mach numbers of 1.2 to 1.4 in the Langley free-flight apparatus.

When several releases of the fin-stabilized nose were made from the airplane model mounted in a vertical nose-down position in the Langley 20-foot free-spinning tunnel, the nose cleared the rear body though sometimes by a narrow margin. When released while the airplane model was free in the tunnel, the nose sometimes cleared the rear body and sometimes hit the wing just as did the unstable nose as mentioned previously. Collision between nose and rear body can probably be avoided by use of forcible forward ejection. A description of an experimental investigation in which forcible forward ejection was used to separate satisfactorily a fin-stabilized nose from a rocket model in flight at a Mach number of 0.87 is presented in reference 9.

CONCLUSIONS

The results of an investigation to determine the motion of a jettisoned nose of a model representative of a transonic research airplane indicate that nose sections without stabilizing fins have an inherent tendency to turn away from a stable nose-first attitude and therefore cause an increased drag which may cause high accelerations on the pilot. The results also indicate that forcible forward ejection of a fin-stabilized jettisonable nose section may be necessary to assure clean separation and to force the nose forward of a region where high negative lift due to the nearness of the rear body may cause high accelerations on the pilot.

Langley Aeronautical Laboratory
National Advisory Committee for Aeronautics
Langley Air Force Base, Va.

REFERENCES

1. Scher, Stanley H.: Wind-Tunnel Investigation of the Stability of Jettisoned Nose Sections of the D-558 Airplane - Phases I and II. NACA RM L7K10, 1948.

2. Gale, Lawrence J.: The Path and Motion of Scale Models of Jettisonable Nose Sections at Supersonic Speeds as Determined from an Investigation in the Langley Free-Flight Apparatus. NACA RM L9J13a, 1950.

3. Scher, Stanley H.: An Empirical Criterion for Fin Stabilizing Jettisonable Nose Sections of Airplanes. NACA RM L9I28, 1949.

4. Goodwin, Roscoe H.: Wind-Tunnel Investigation at Low Speed to Determine the Aerodynamic Properties of a Jettisonable Nose Section with Circular Cross Section. NACA RM L9J13, 1950.

5. Scherberg, Max, and Rhode, R. V.: Mass Distribution and Performance of Free Flight Models. NACA TN 268, 1927.

6. Shortal, Joseph A., and Osterhout, Clayton J.: Preliminary Stability and Control Tests in the NACA Free-Flight Wind Tunnel and Correlation with Full-Scale Flight Tests. NACA TN 810, 1941.

7. Zimmerman, C. H.: Preliminary Tests in the N.A.C.A. Free-Spinning Wind Tunnel. NACA Rep. 557, 1936.

8. Lombard, Charles F.: How Much Force Can Body Withstand? Aviation Week, vol. 50, no. 3, Jan. 17, 1949, pp. 20-28.

9. Lundstrom, Reginald R., and O'Kelly, Burke R.: Flight Investigation of the Jettisonable-Nose Method of Pilot Escape Using Rocket-Propelled Models. NACA RM L9D11, 1949.

TABLE I.- MASS CHARACTERISTICS OF A $\frac{1}{25}$-SCALE MODEL REPRESENTATIVE

OF A TRANSONIC AIRPLANE AND ITS JETTISONABLE NOSE SECTION

[Model values converted to corresponding full-scale values; moments of inertia are given about center-of-gravity locations of airplane and nose, respectively.]

Configuration	Weight (lb)	Center-of-gravity location	Moments of inertia (slug-ft^2)		
			I_X	I_Y	I_Z
Airplane model, including nose	11,182	20.5 percent of mean aerodynamic chord	3024	30,167	32,158
Nose model	766	Approximately 66 percent of length of nose (front to back)	33	108	108

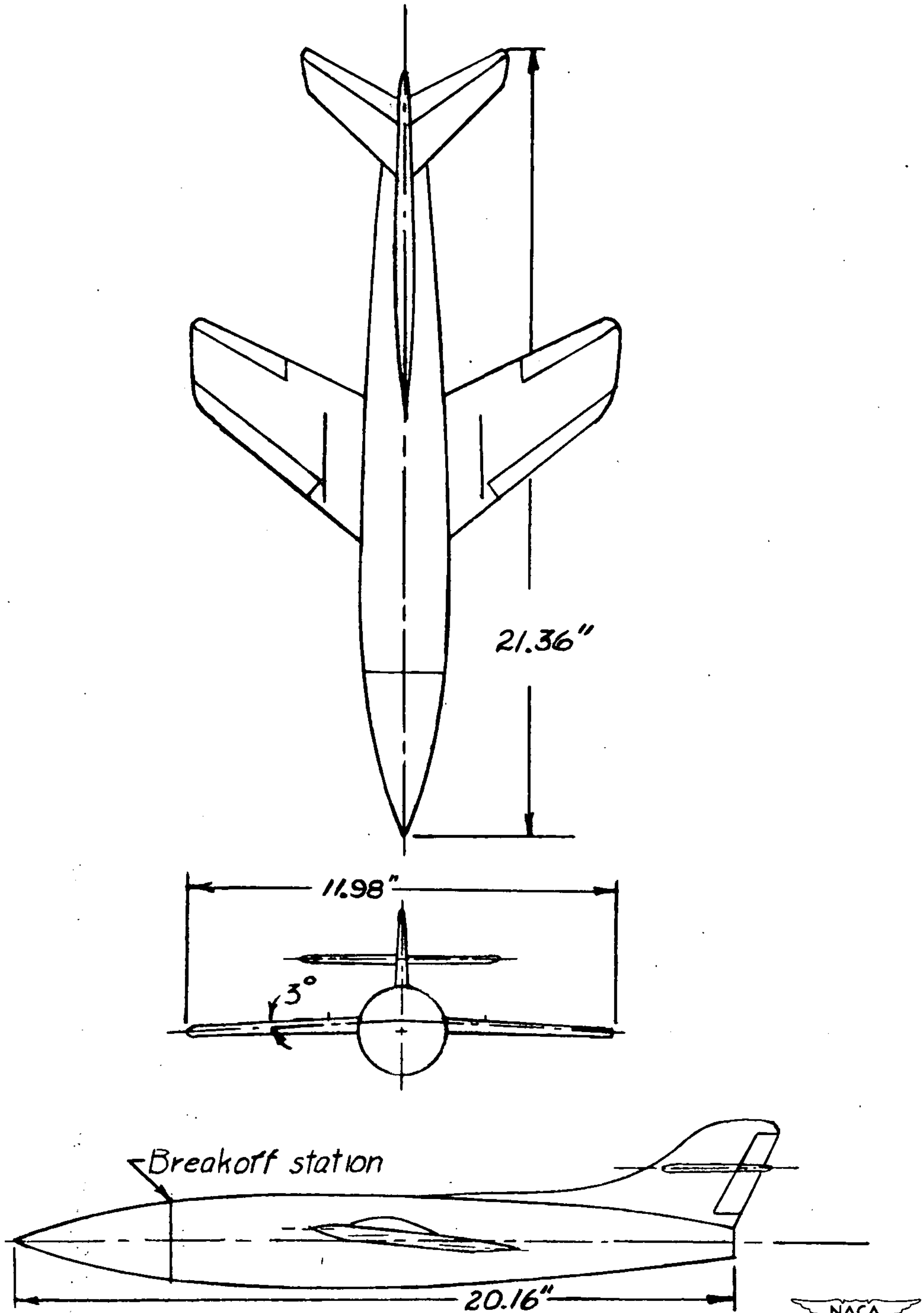

Figure 1.- Three-view drawing of the $\frac{1}{25}$-scale model of a representative transonic airplane used in the nose-release investigation.

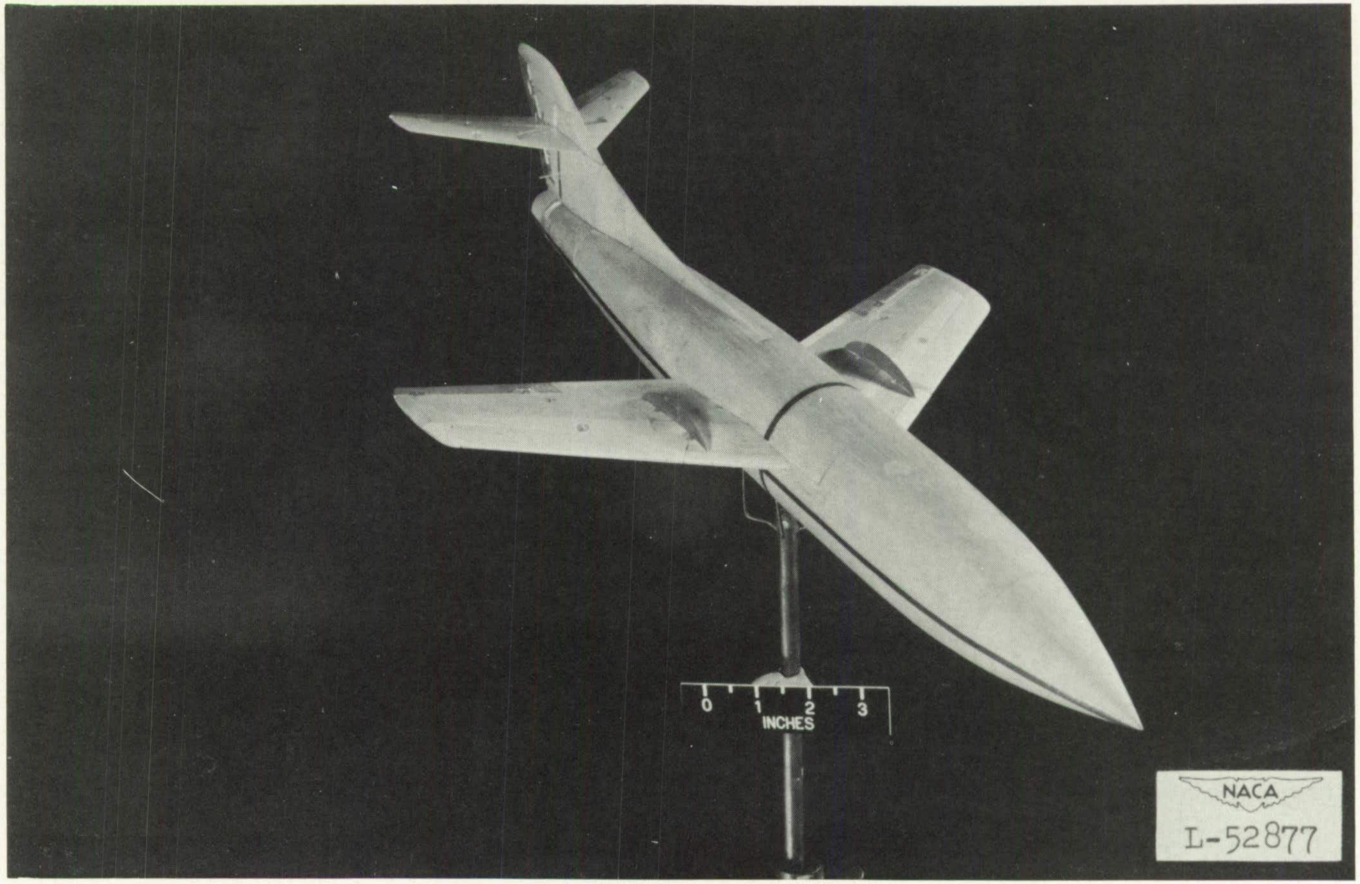

Figure 2.- The $\frac{1}{25}$-scale model of a representative transonic airplane used in the nose-release investigation.

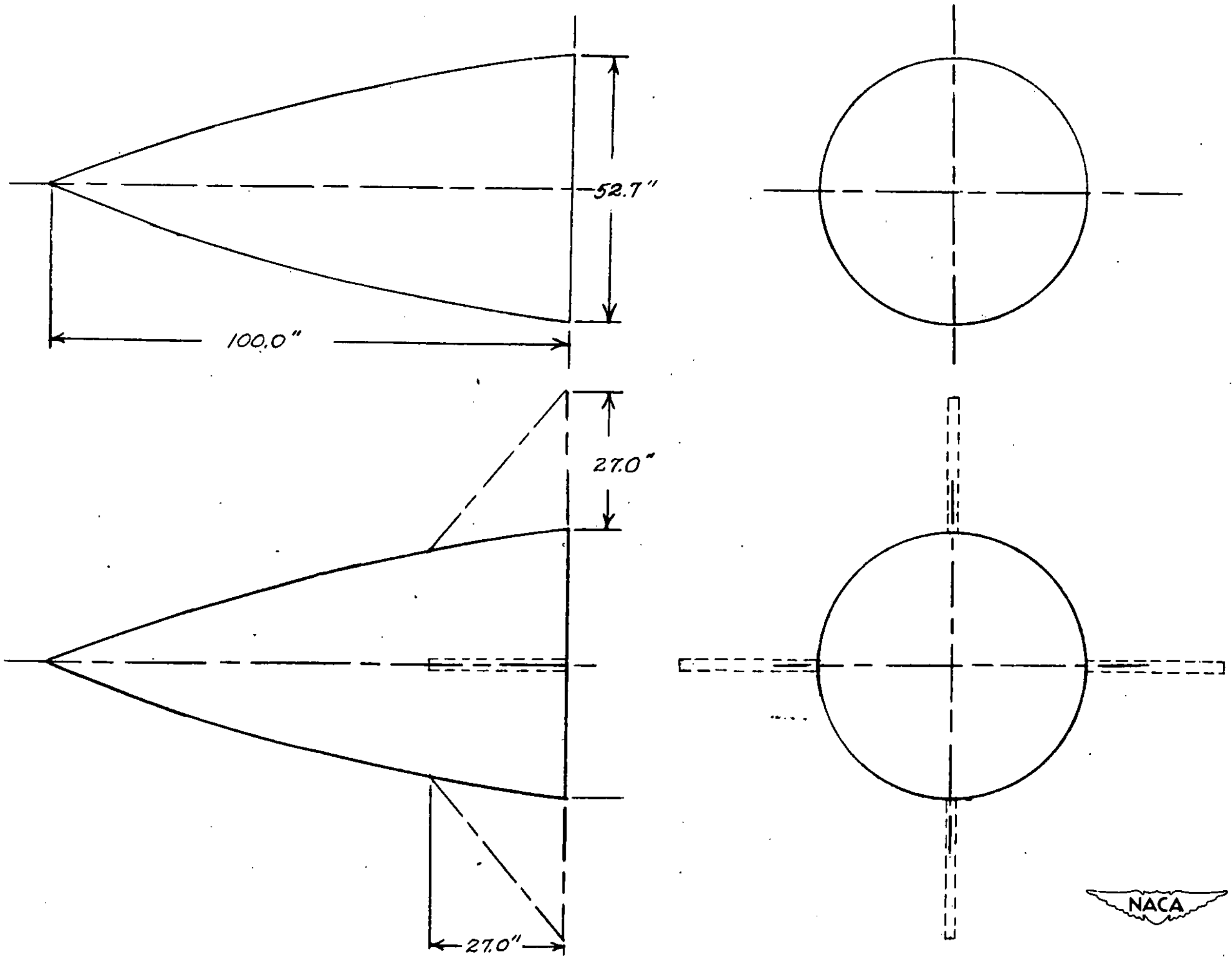

Figure 3.- Sketches of the $\frac{1}{25}$-scale model of the jettisonable nose of the representative transonic airplane. Nose is shown with and without stabilizing fins. Dimensions are full-scale values.

Figure 4.- Motion-picture strips of unstable nose release at 80 miles per hour (400 mph, full scale) in the Langley 300 MPH 7- by 10-foot tunnel.

L-63058

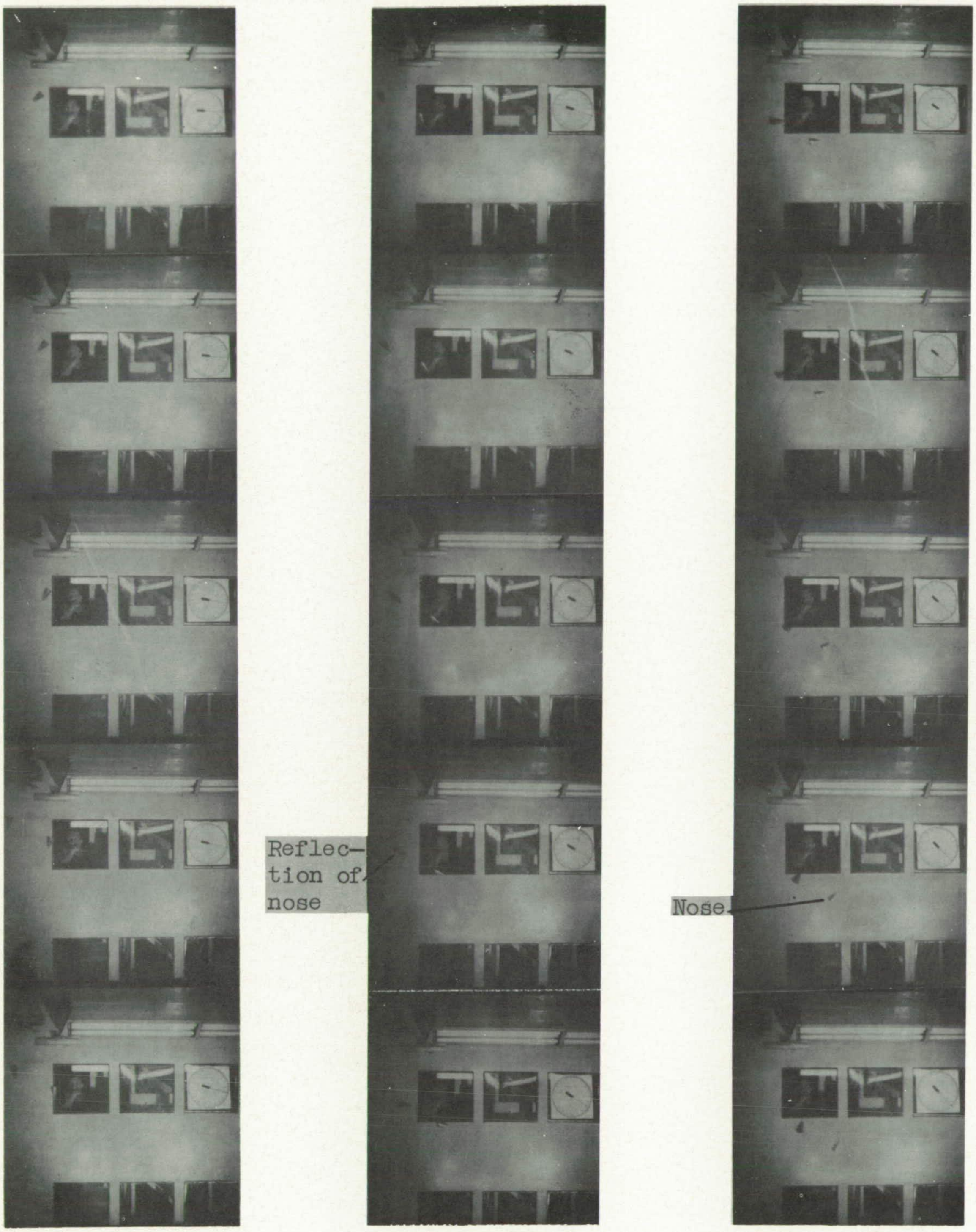

Figure 4.– Continued.

NACA
L-63059

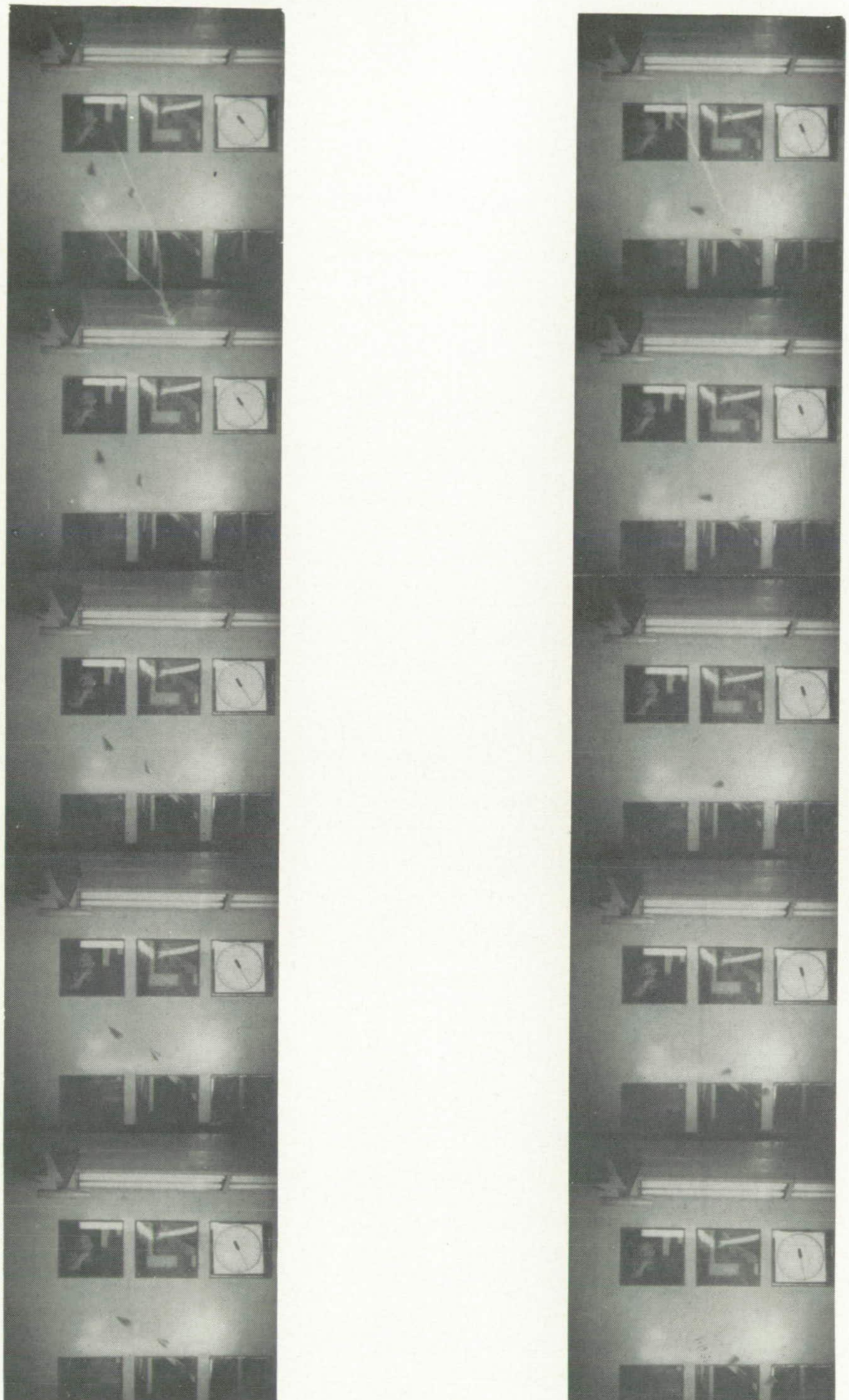

Figure 4.- Concluded.

L-63060

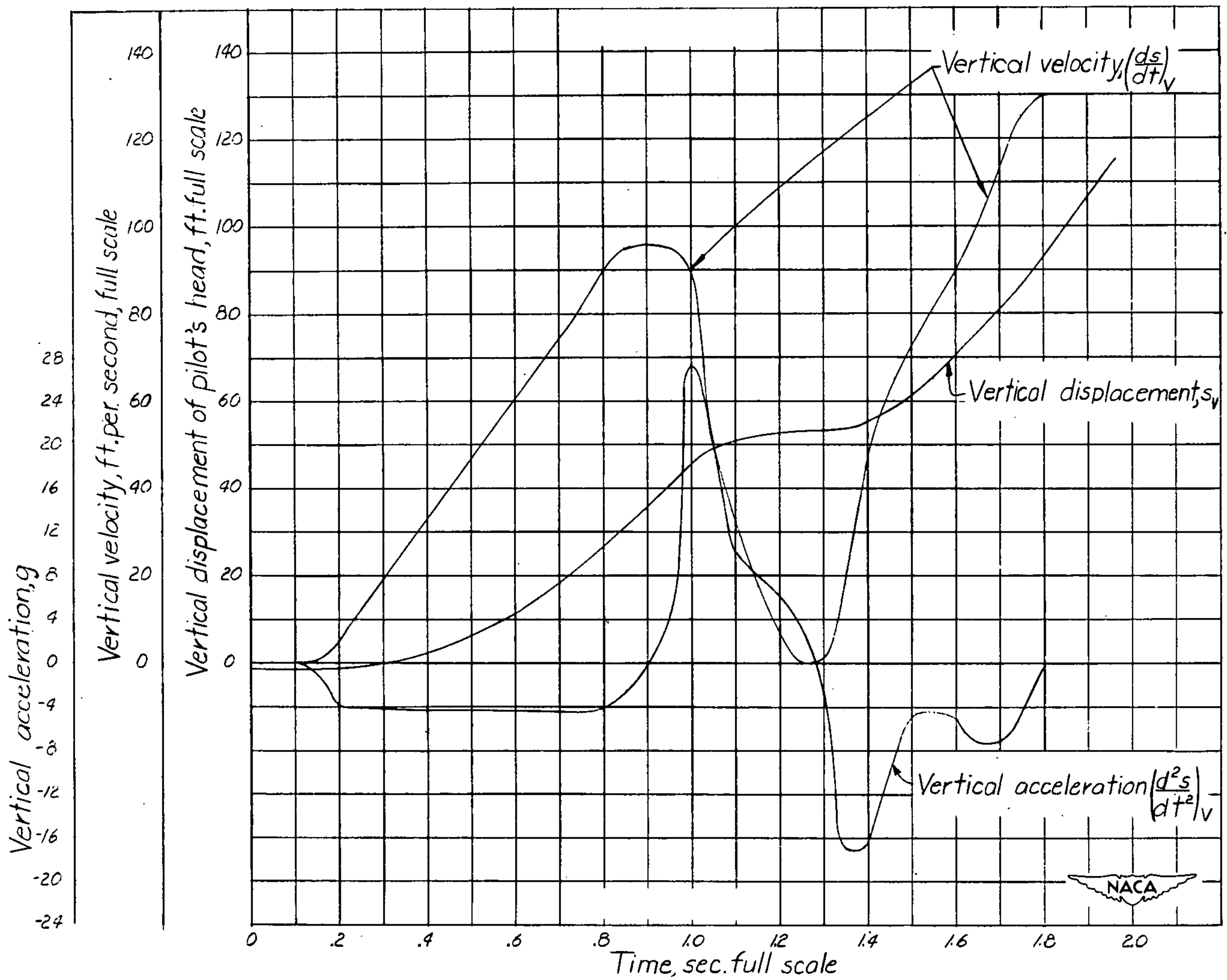

(a) Vertical.

Figure 5.– Variation of vertical and horizontal displacement, velocity, and acceleration with time for nose section not stabilized with fins when released at 80 miles per hour (400 mph, full scale).

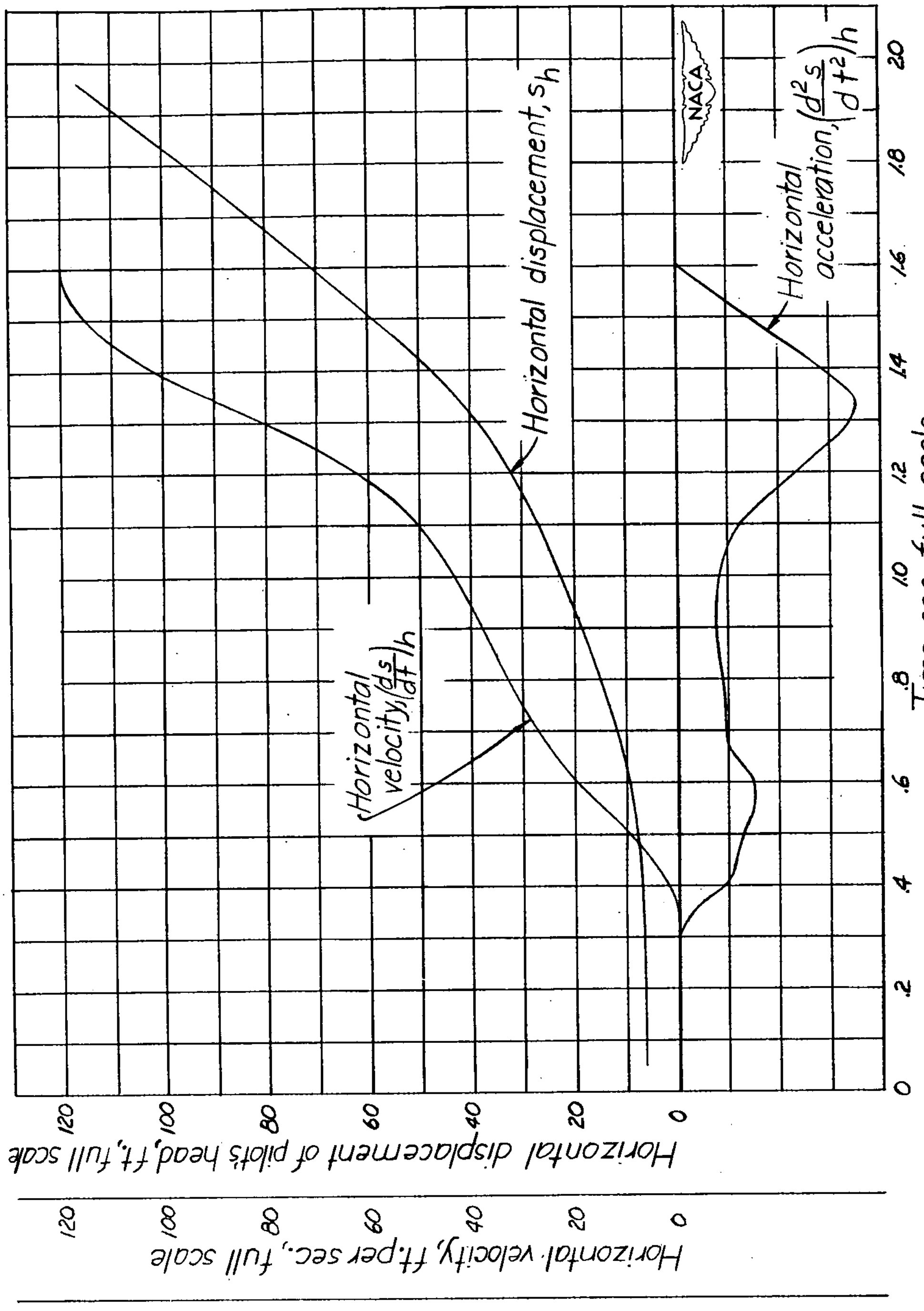

(b) Horizontal.

Figure 5.- Concluded.

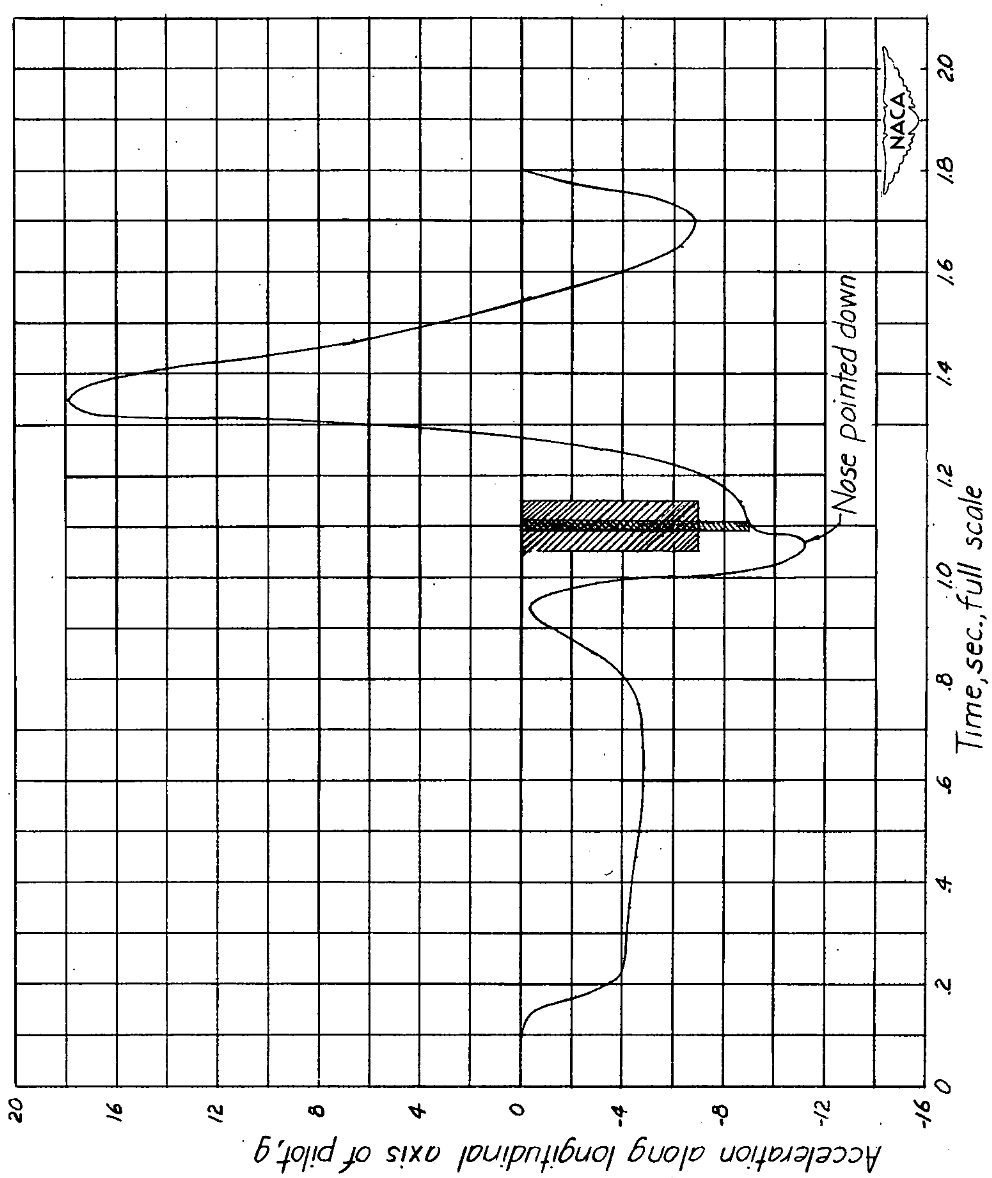

Figure 6.– Variation of acceleration along pilot's backbone with time for nose section not stabilized with fins when released at 80 miles per hour (400 mph, full scale). Cross hatching indicates limits of human tolerance to acceleration, as obtained from reference 8.

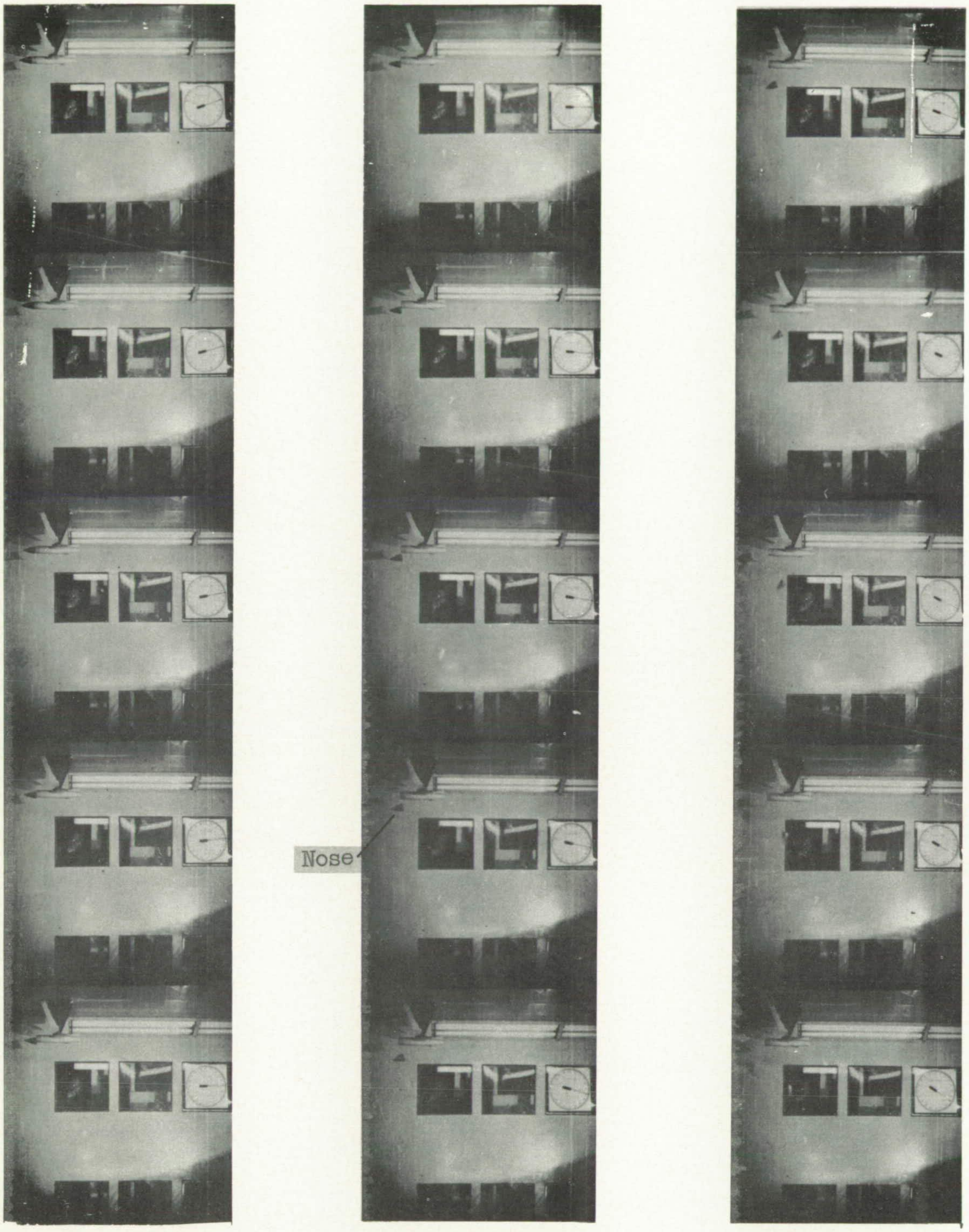

Figure 7.- Motion-picture strips of unstable nose release at 125 miles per hour (625 mph, full scale) in the Langley 300 MPH 7- by 10-foot tunnel.

L-63061

Figure 7.– Concluded.

L-63062

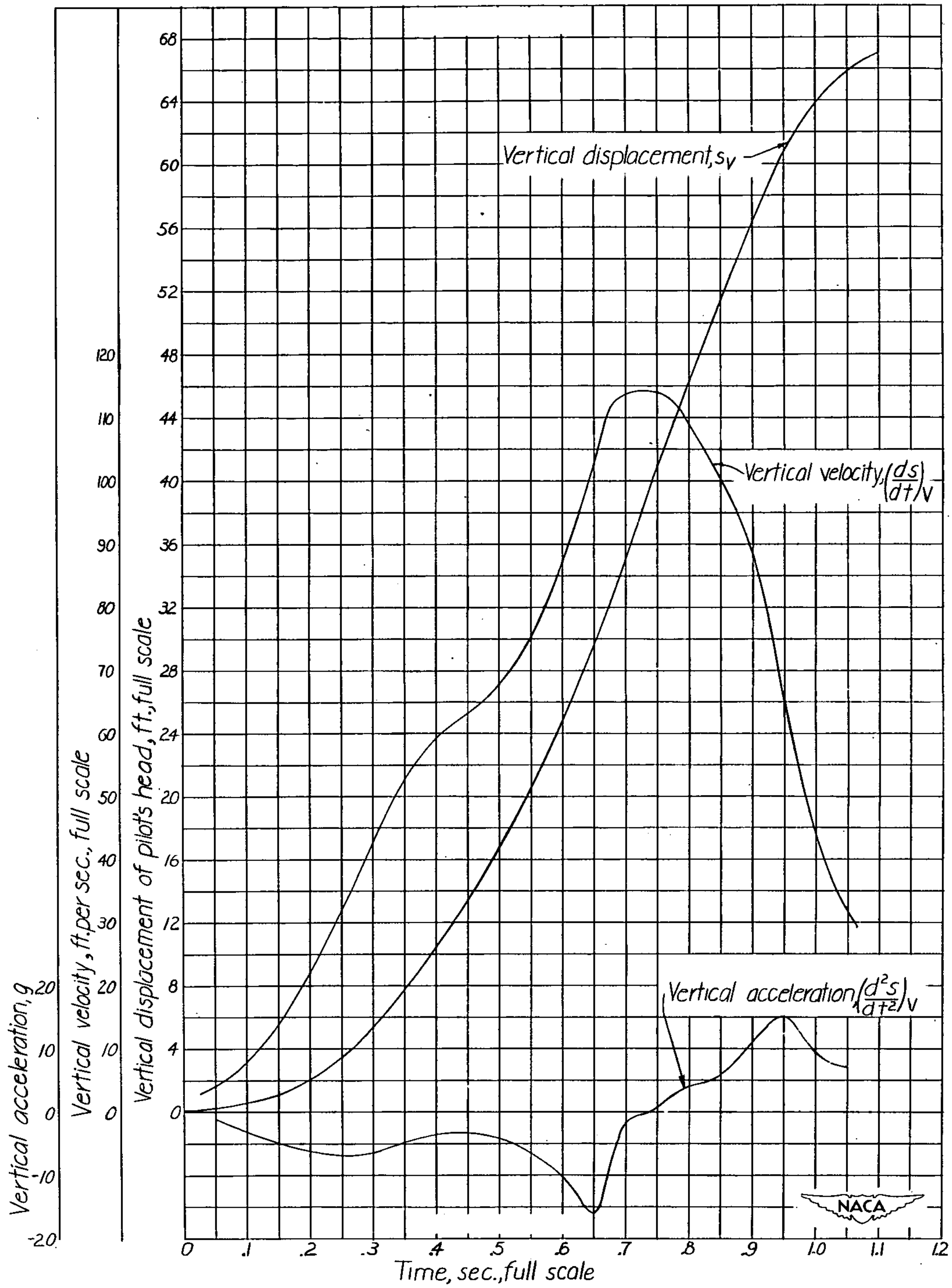

(a) Vertical.

Figure 8.- Variation of vertical and horizontal displacement, velocity, and acceleration with time for nose section not stabilized with fins when released at 125 miles per hour (625 mph, full scale).

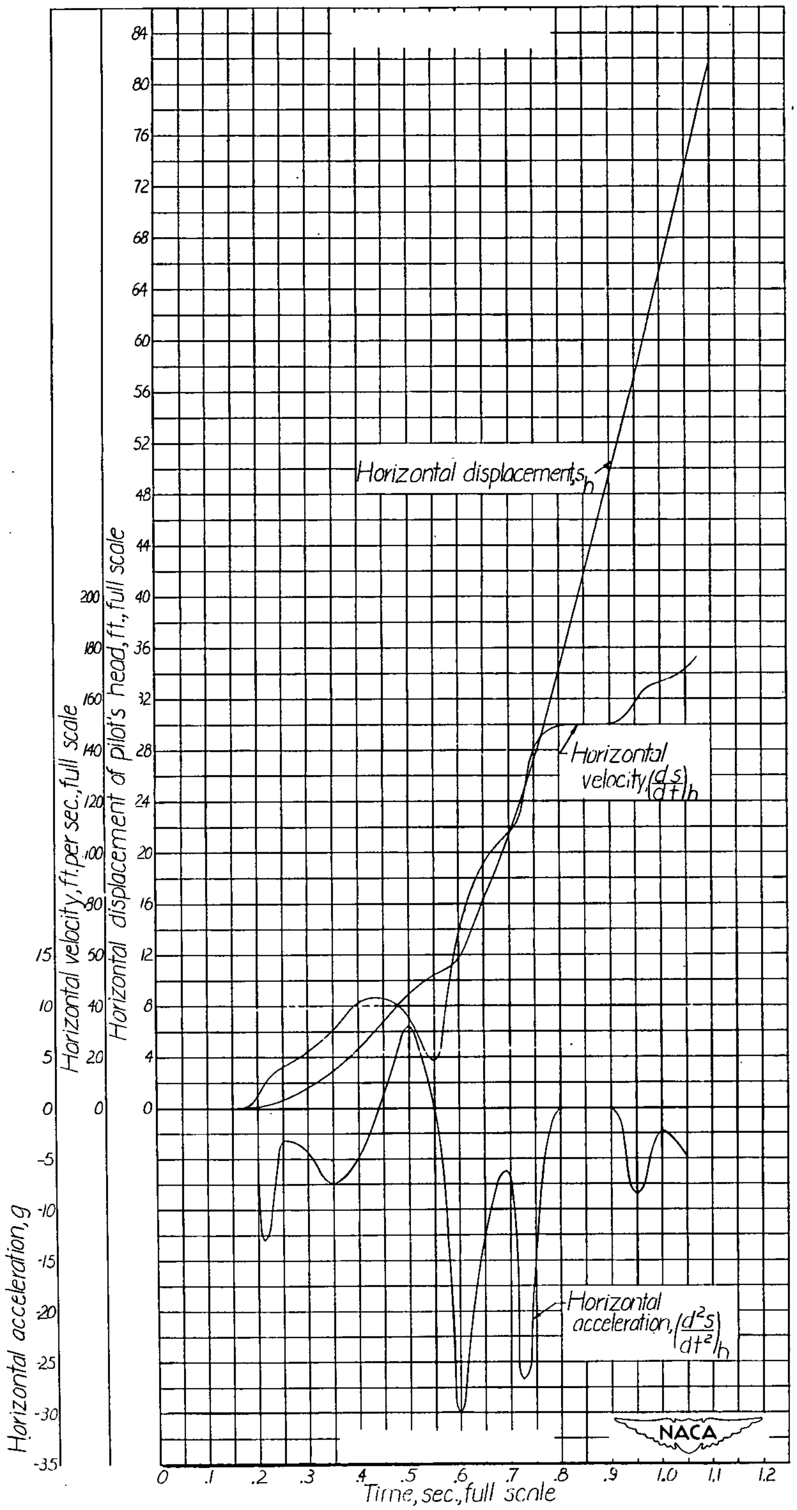

(b) Horizontal.

Figure 8.— Concluded.

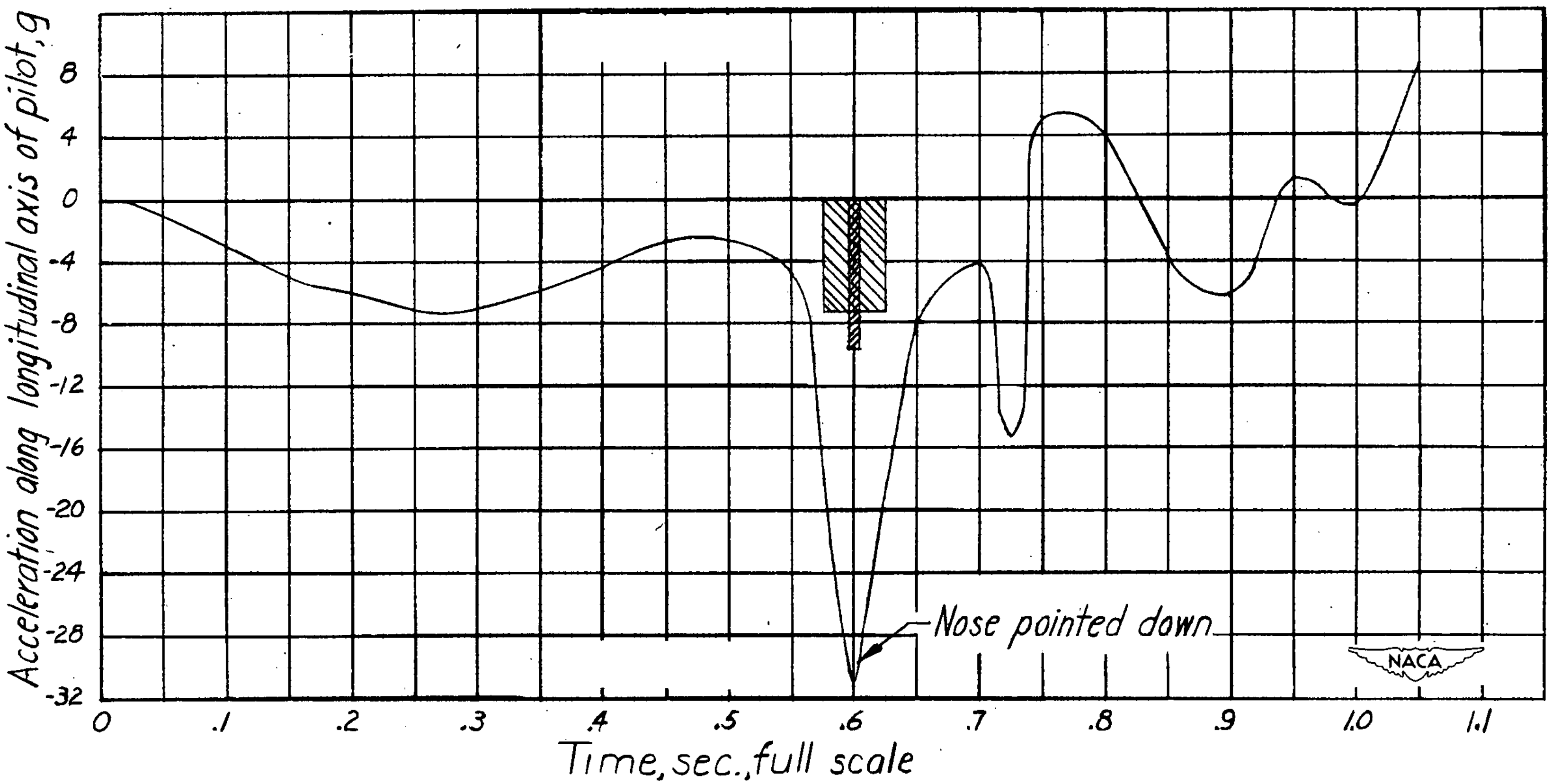

Figure 9.– Variation of acceleration along pilot's backbone with time for nose section not stabilized with fins when released at 125 miles per hour (625 mph, full scale). Cross hatching indicates limits of human tolerance to acceleration, as obtained from reference 8.

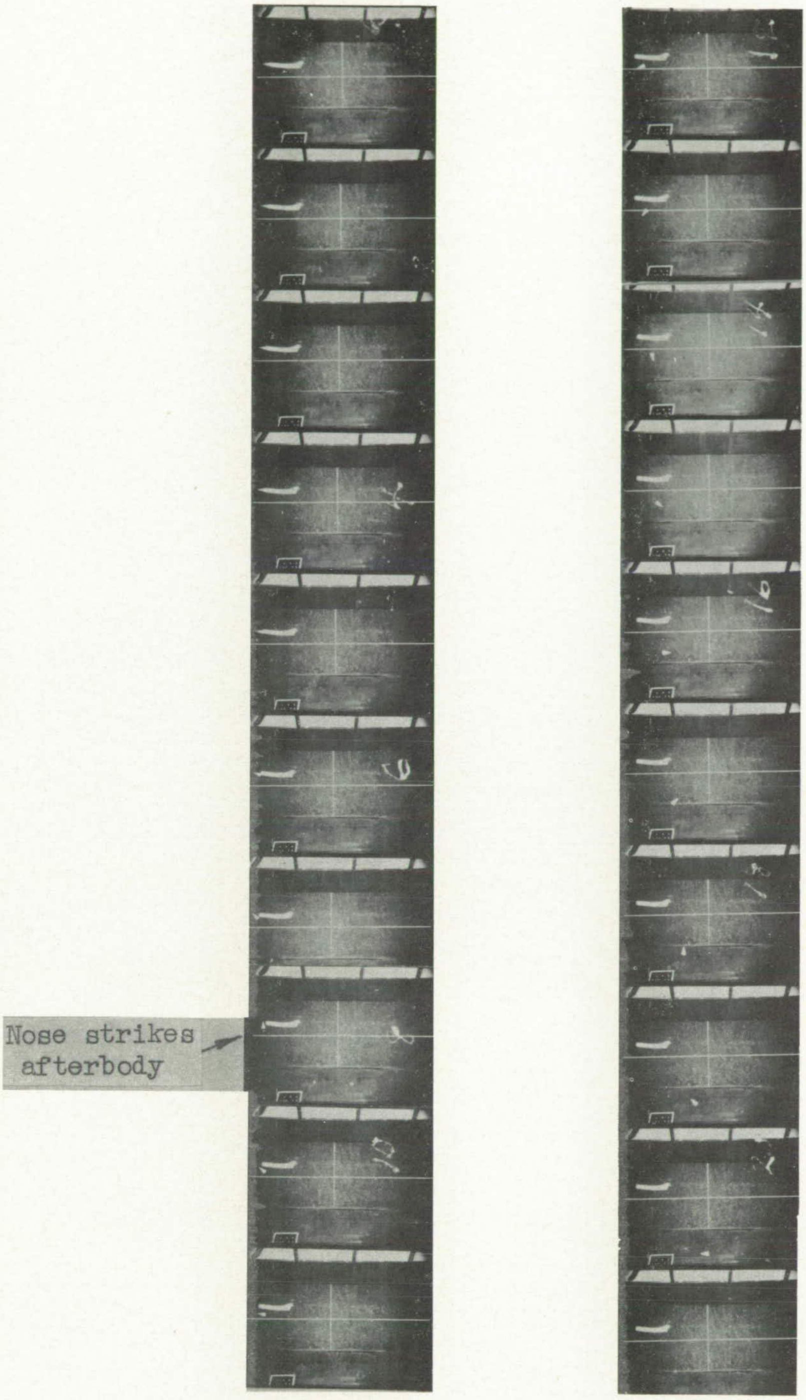

Figure 10.- Motion-picture strips of unstable nose release in the Langley free-flight tunnel. Simulated 30° gliding flight, angle of attack is 8°.

L-63069

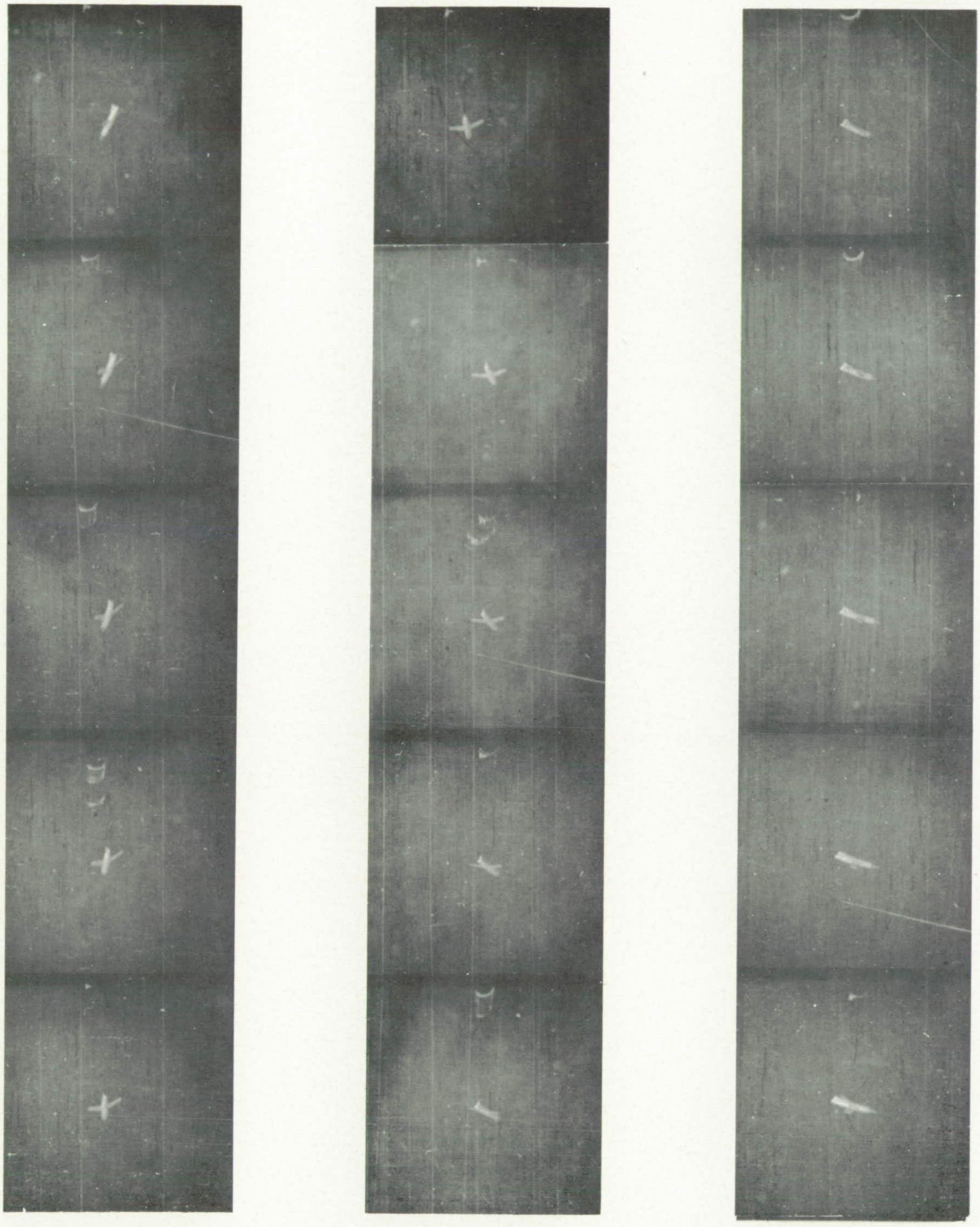

Figure 11.- Motion pictures of unstable nose release from model without tail in the Langley 20-foot free-spinning tunnel.

NACA
L-63063

Figure 11.- Continued.

NACA
L-63064

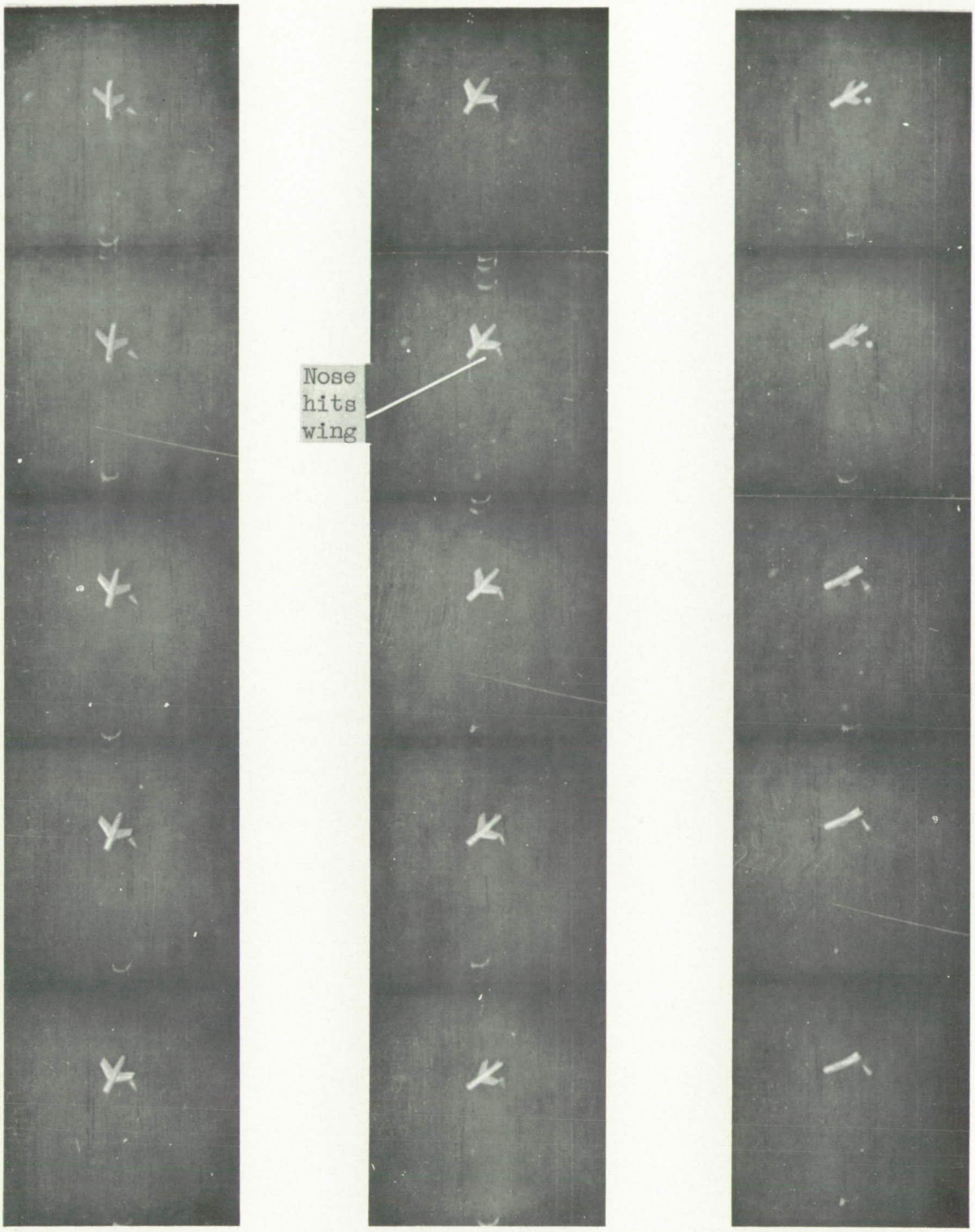

Figure 11.- Continued.

L-63065

Figure 11.- Continued.

NACA
L-63066

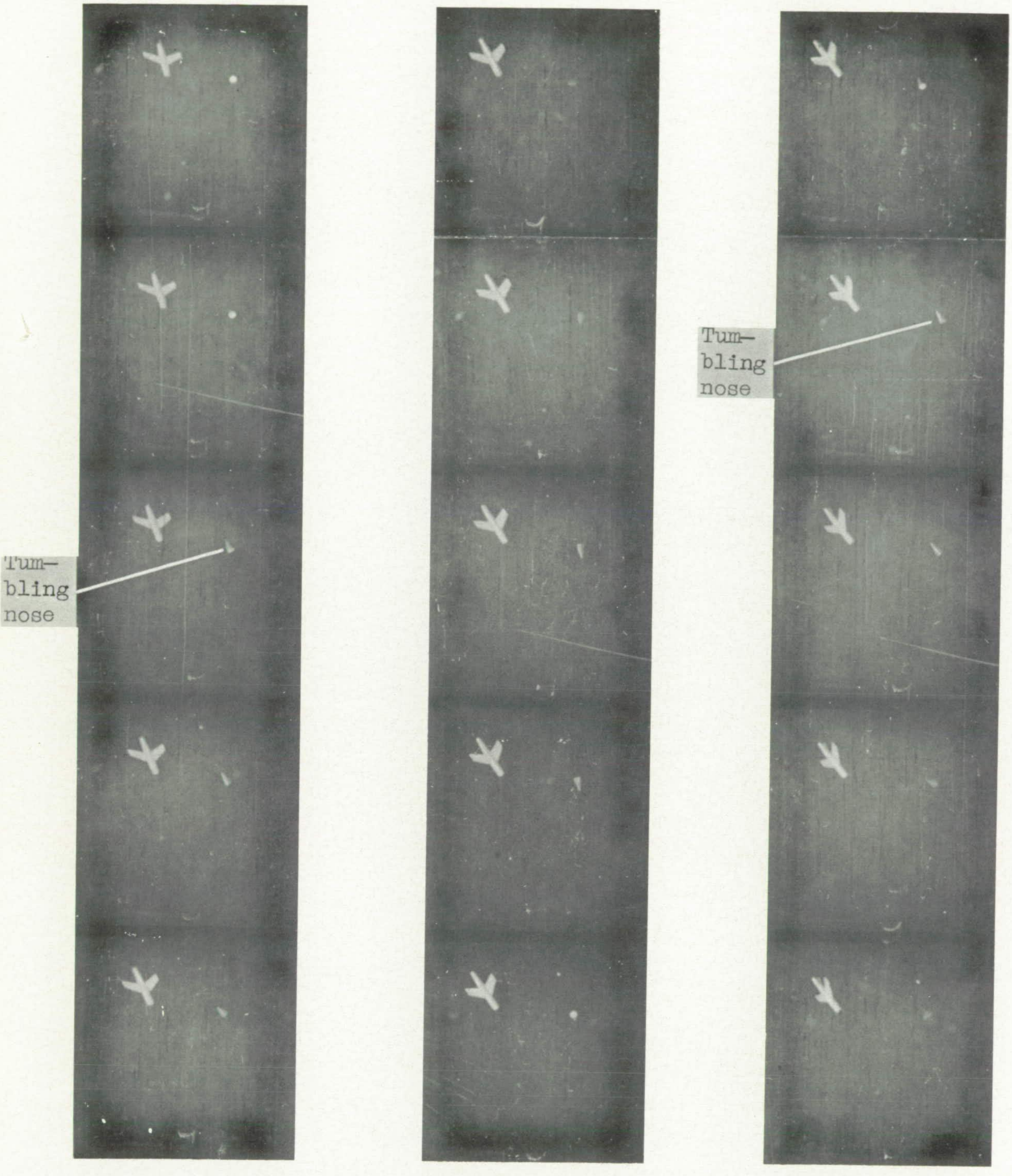

Figure 11.- Continued.

NACA
L-63067

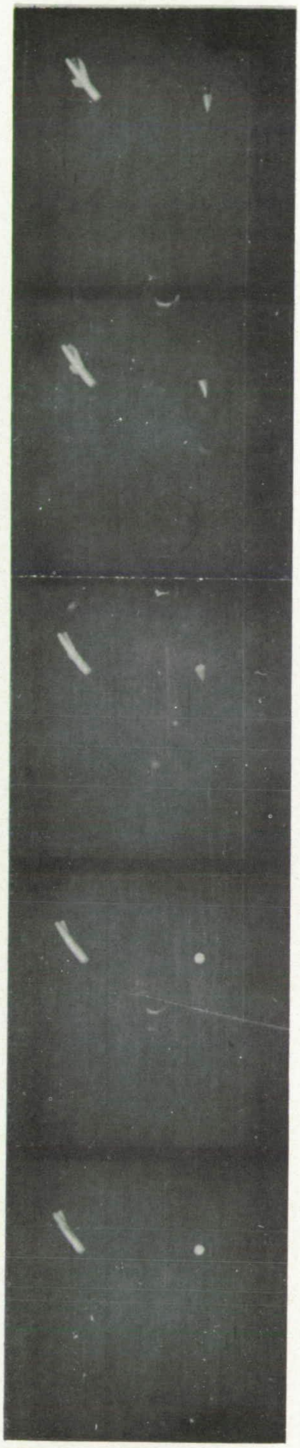

Figure 11.- Concluded.

NACA
L-63068

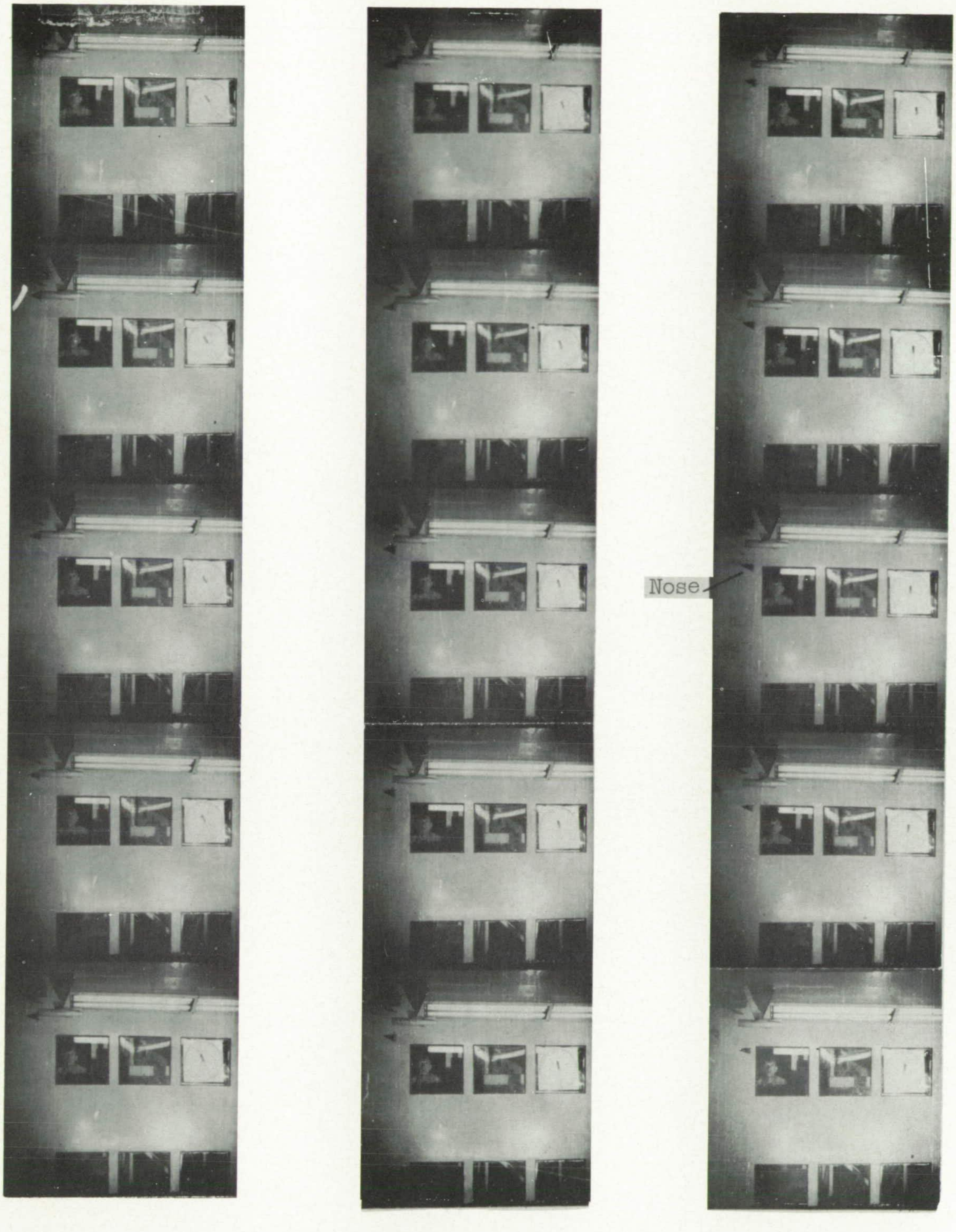

Figure 12.- Motion-picture strips of fin-stabilized nose release at 80 miles per hour (400 mph, full scale) in the Langley 300 MPH 7- by 10-foot tunnel.

L-63070

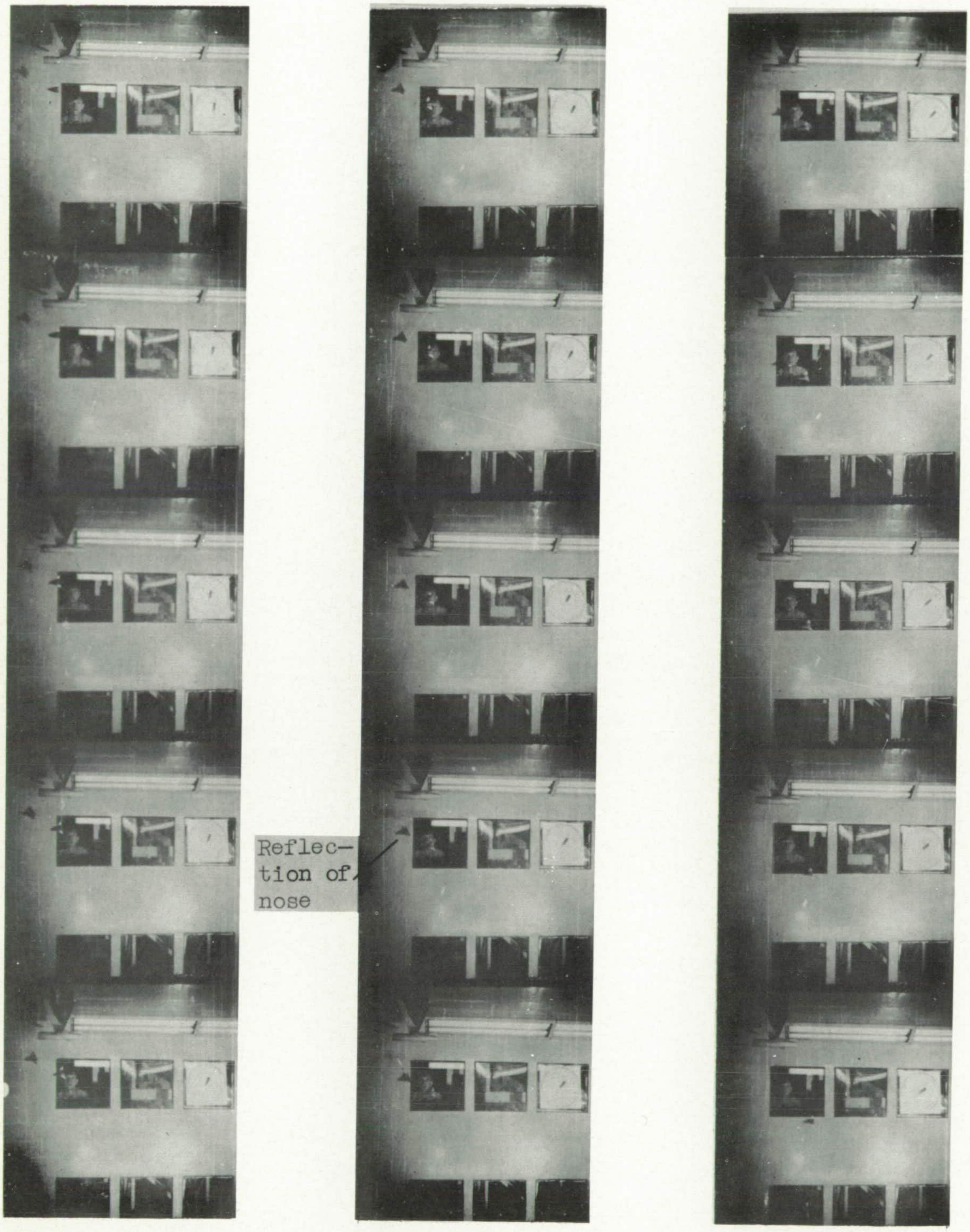

Figure 12.- Continued.

NACA
L-63071

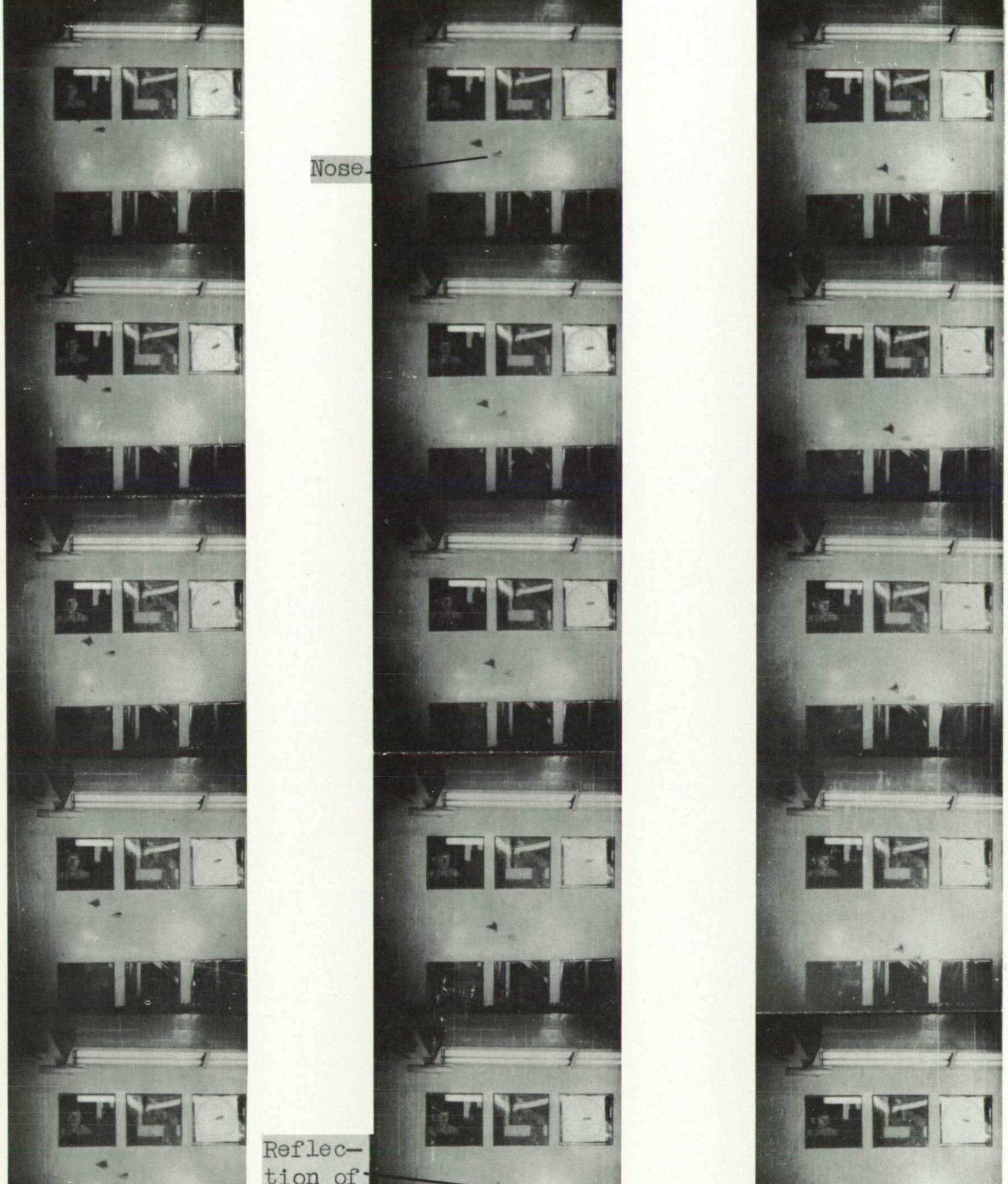

Figure 12.- Continued.

L-63072

Figure 12.- Concluded.

L-63073

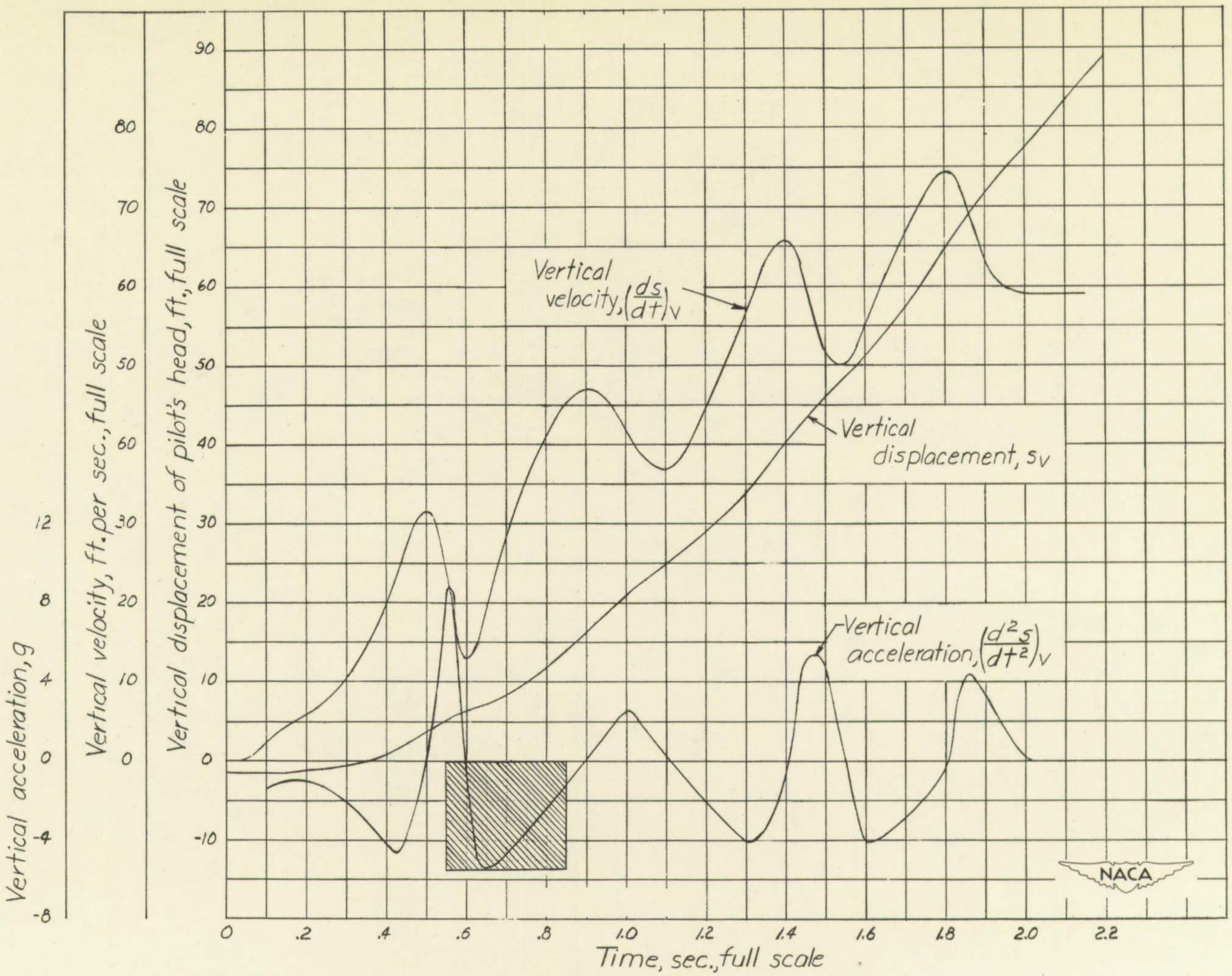

(a) Vertical.

Figure 13.- Variation of vertical and horizontal displacement, velocity, and acceleration with time for fin-stabilized nose release at 80 miles per hour (400 mph, full scale). Cross hatching indicates limits of human tolerance to acceleration, as obtained from reference 8.

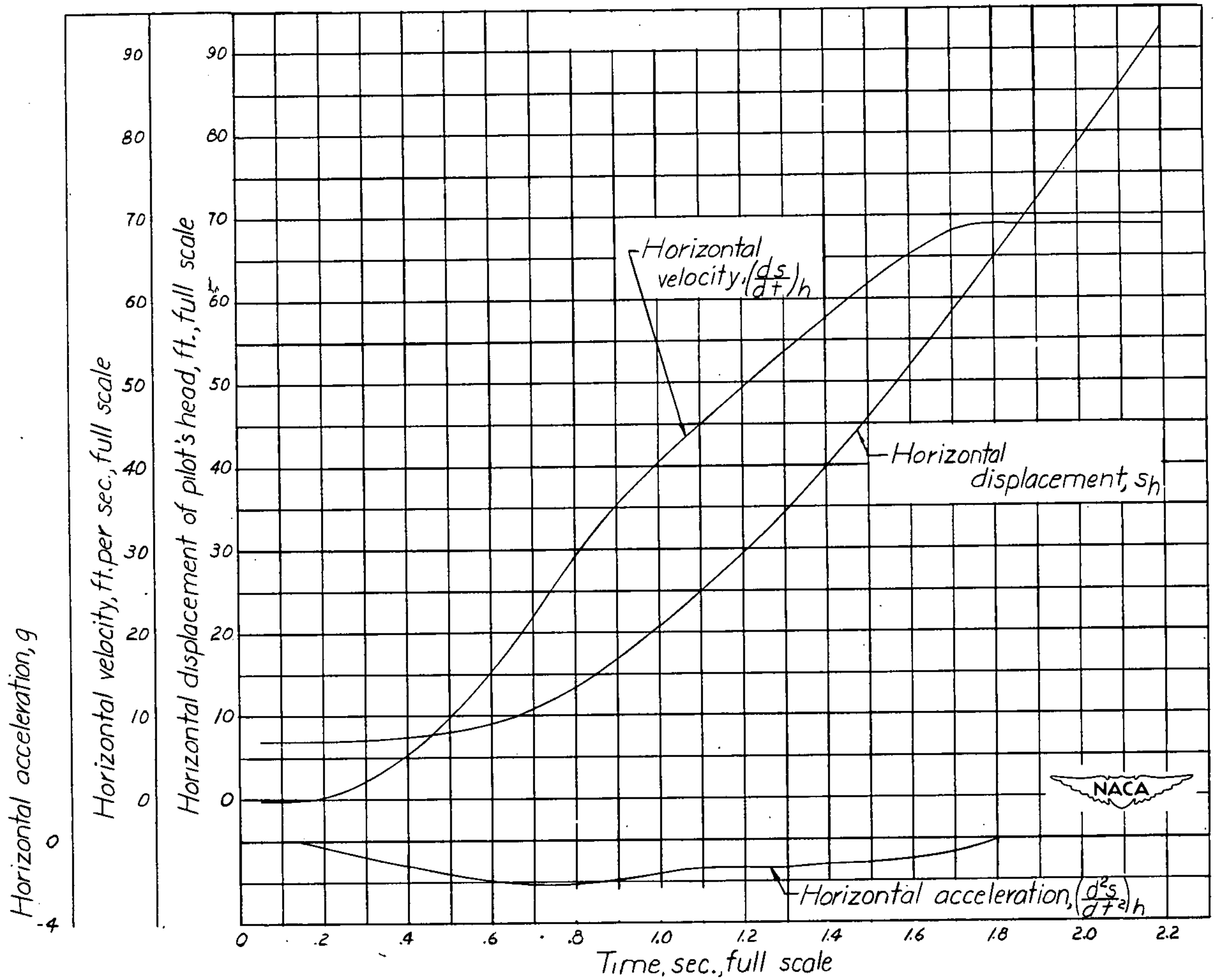

(b) Horizontal.

Figure 13.- Concluded.

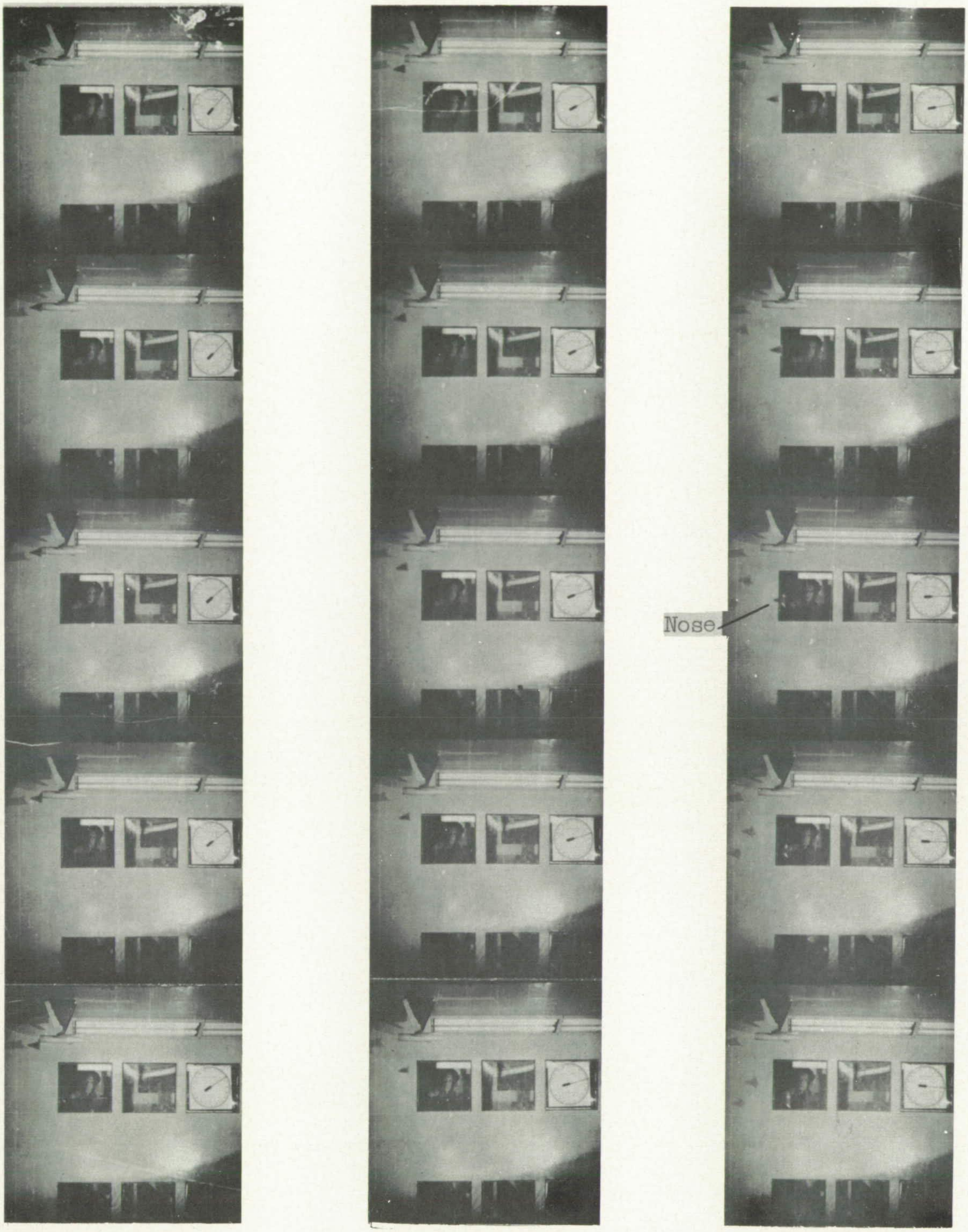

Figure 14.- Motion-picture strips of fin-stabilized nose release at 125 miles per hour (625 mph, full scale) in the Langley 300 MPH 7- by 10-foot tunnel.

NACA

L-63074

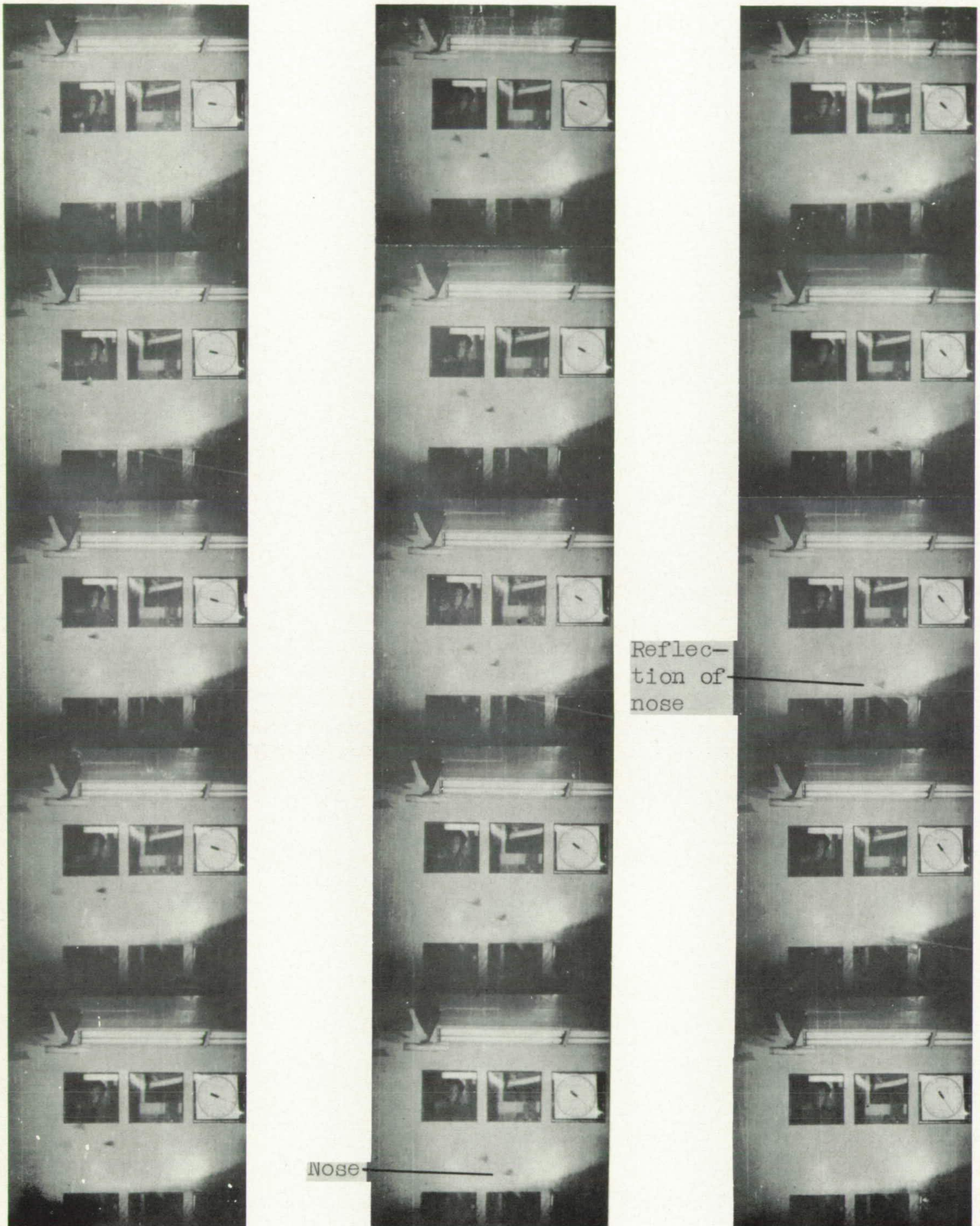

Figure 14.- Concluded.

L-63075

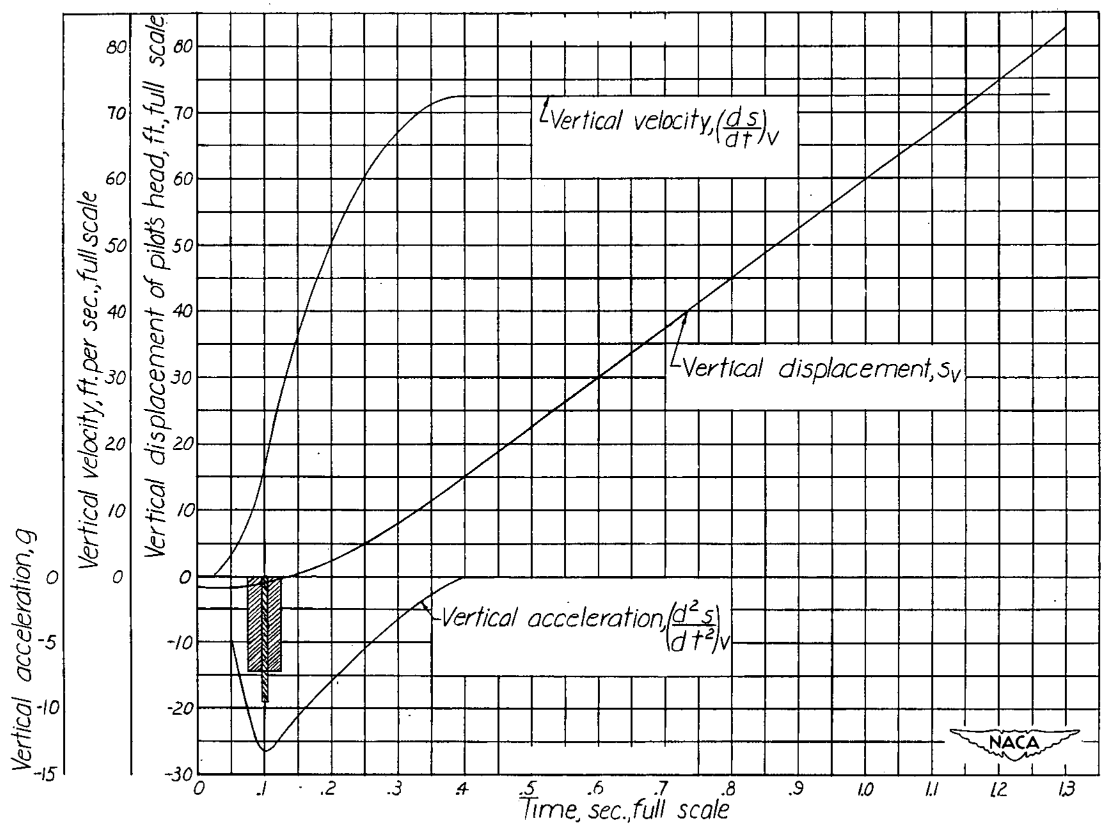

(a) Vertical.

Figure 15.- Variation of vertical and horizontal displacement, velocity, and acceleration with time for fin-stabilized nose release at 125 miles per hour (625 mph, full scale). Cross hatching indicates limits of human tolerance to acceleration, as obtained from reference 8.

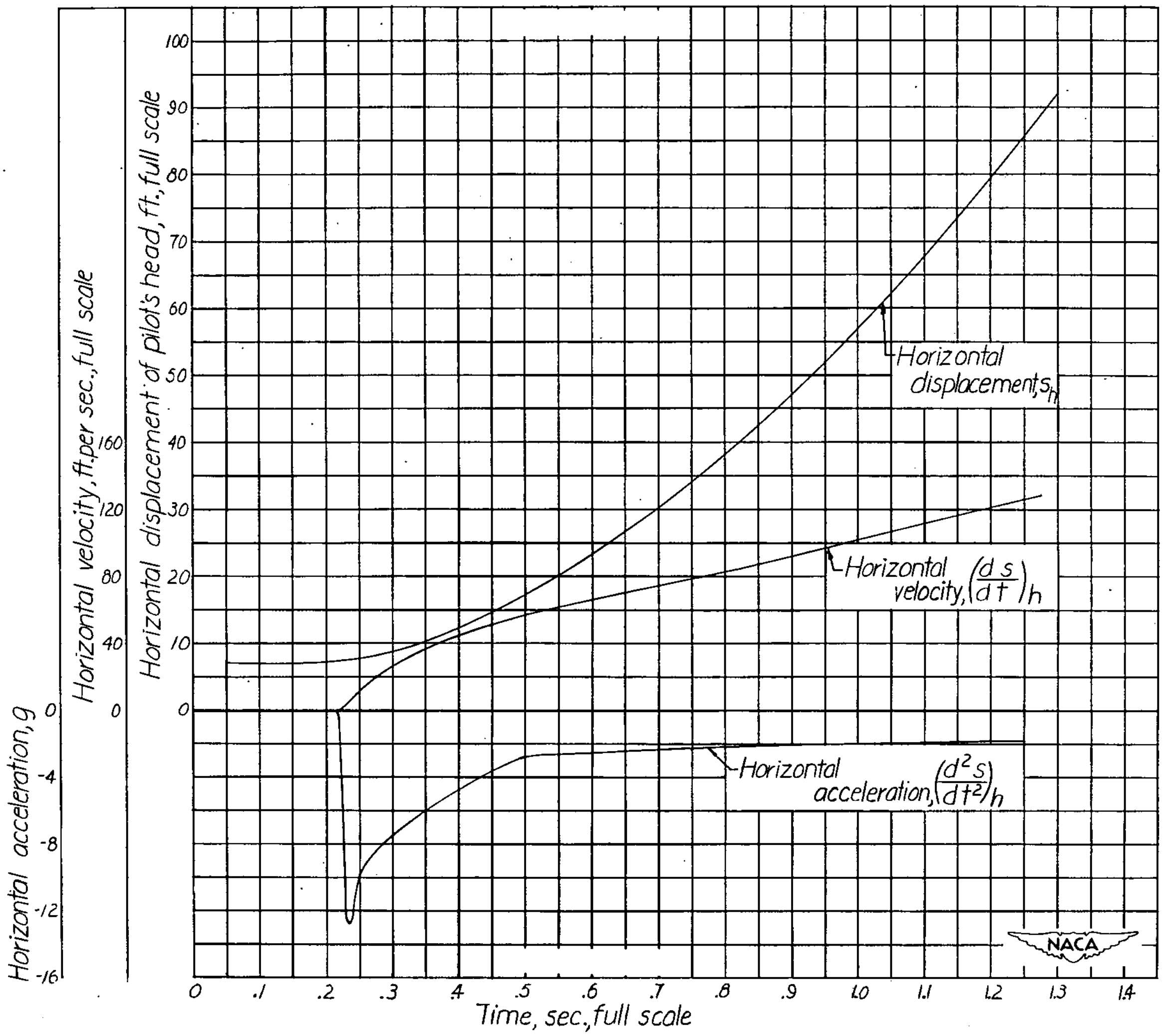

(b) Horizontal.

Figure 15.- Concluded.